

---

# Force Control of Robotic Walker

---

## UNDERGRADUATE THESIS

*Submitted in partial fulfillment of the requirements of  
BITS F421T Thesis*

*By*

Kunal GUPTA  
ID No. 2014A3TS0188P

*Under the supervision of:*

Dr. YU HAOYONG  
&  
Dr. Surekha BHANOT



BIRLA INSTITUTE OF TECHNOLOGY AND SCIENCE PILANI, PILANI CAMPUS  
December 2017

# **Declaration of Authorship**

I, Kunal GUPTA, declare that this Undergraduate Thesis titled, ‘Force Control of Robotic Walker’ and the work presented in it are my own. I confirm that:

- This work was done wholly or mainly while in candidature for a research degree at this University.
- Where any part of this thesis has previously been submitted for a degree or any other qualification at this University or any other institution, this has been clearly stated.
- Where I have consulted the published work of others, this is always clearly attributed.
- Where I have quoted from the work of others, the source is always given. With the exception of such quotations, this thesis is entirely my own work.
- I have acknowledged all main sources of help.
- Where the thesis is based on work done by myself jointly with others, I have made clear exactly what was done by others and what I have contributed myself.

Signed:

---

Date:

---

# Certificate

This is to certify that the thesis entitled, “*Force Control of Robotic Walker*” and submitted by Kunal GUPTA ID No. 2014A3TS0188P in partial fulfillment of the requirements of BITS F421T Thesis embodies the work done by him under my supervision.

---

*Supervisor*

Dr. YU HAOYONG  
Associate Professor,  
National University of Singapore  
Date:

---

*Co-Supervisor*

Dr. Surekha BHANOT  
Professor,  
BITS-Pilani Pilani Campus  
Date:

*“Only those who will risk going too far can possibly find out how far one can go.”*

T. S. Eliot

BIRLA INSTITUTE OF TECHNOLOGY AND SCIENCE PILANI, PILANI CAMPUS

## *Abstract*

Bachelor of Engineering (Hons.)

### **Force Control of Robotic Walker**

by Kunal GUPTA

This thesis address the problem of safety in the overground robotic walkers. The overground robotic walkers are a particular type of robotic gait rehabilitation devices where the patient can walk freely over the ground while the walker provides the necessary body weight support. For robotic gait rehabilitation devices, it is extremely important to ensure the safety of the patient using the device. There are mainly two types of safety issues concerning the overground robotic walker. Firstly, the admittance control which is used for intuitive human-walker interaction needs to be stable which means the absence of any kind of undamped oscillations. Secondly, the walker needs to provide adequate support to the patient during the gait instability to prevent falls. In this work, a thorough stability analysis of the admittance control is performed and appropriate bounds on the admittance parameters are derived. A novel ‘Stable Gait criterion’(SGC) is proposed which has been demonstrated to be an extremely reliable method for the detection of gait instability. A support scheme based on the idea of ‘Force-Tunnel’ is also proposed. The safety control consisting of SGC and force-tunnel is tested on five subjects and results have shown high sensitivity and specificity of the controller. With the proposed safety control the overground walker is able to deliver sufficient support to the patient and prevent fall instances.

## *Acknowledgements*

First of all, I would like to express my gratitude to my thesis supervisor, Dr. YU Haoyong. I would like to thank him for giving me an opportunity to work in the Advanced Robotic Center at the prestigious National University of Singapore, as part of the BioRobotics Lab. Due to his able guidance, I was able to channelize my efforts constructively to solve a major obstacle to the development of the overground robotic walker.

I am deeply indebted to Dr. Gabriel Aguirre Ollinger for his technical suggestions in my project. During my brief stay in NUS, I have learned invaluable lessons from Dr. Gabriel about the practical implementation of control systems. It is due to his vast knowledge and several years of experience that helped me to overcome key challenges during my research.

I would also like to thank Ashwin Narayan for being a constant source of motivation. I would like to thank him for being a great friend, for always boosting up my confidence when I felt low. I would also like to thank him to teach me how to systematically tackle complex problems in research.

I would also like to thank Francisco Anaya and Hsiao-Ju Cheng for their valuable insights into the medical aspects of the walker. Their experience in working with stroke patients helped make my research more practical.

I am grateful to my co-supervisor, Dr. Surekha Bhanot for agreeing to supervise my thesis. I cannot thank her enough for her constant encouragement and support that propelled me to explore deeper topics in robotics during my undergraduate studies.

I would like to thank all my colleagues from BioRobotics Lab for making my brief stay in Singapore a wonderful experience. I would never forget the moments we spent together.

Lastly, I would like to thank my family for bravely standing by my side as I take the road less travelled.

# Contents

<b>Declaration of Authorship</b>	i
<b>Certificate</b>	ii
<b>Abstract</b>	iv
<b>Acknowledgements</b>	v
<b>Contents</b>	vi
<b>List of Figures</b>	viii
<b>1 Introduction</b>	1
1.1 Problem Statement and Research Challenges . . . . .	3
1.2 Contributions . . . . .	4
1.3 Thesis Structure . . . . .	5
<b>2 Related Work</b>	6
2.1 Force Control . . . . .	6
2.1.1 Indirect Force Control . . . . .	7
2.1.2 Direct Force Control . . . . .	7
2.1.2.1 Explicit Force control . . . . .	7
2.1.2.2 Implicit Force control . . . . .	8
2.2 Safety Control . . . . .	8
<b>3 Robotic Walker</b>	9
3.1 Omni-Directional Platform . . . . .	10
3.2 Linear Drive . . . . .	10
3.3 Sensors. . . . .	11
<b>4 Walker Kinematics</b>	12
4.1 Sign Convention . . . . .	12
4.2 Wheel Kinematics . . . . .	13
4.3 Platform Kinematics . . . . .	15

<b>5 Admittance Control of Walker</b>	<b>16</b>
5.1 Walker Velocity Transfer function.	17
5.2 Human-Walker interaction model	18
5.3 Human-Walker System block diagram.	19
5.4 Stability Analysis of Human-Walker system.	19
<b>6 State Estimation</b>	<b>23</b>
6.1 State Estimation: Kalman Filter	23
<b>7 Safety Control of Walker</b>	<b>27</b>
7.1 Force Tunnel	27
7.2 Safety-Zone Criterion	28
7.2.1 Control Scheme for Safety Zone	29
7.2.1.1 Calculation of parameters	30
7.3 Comments on Safety Zone	31
7.4 Stable Gait criterion	32
<b>8 Results</b>	<b>38</b>
8.1 Response time.	39
8.2 Critical distance.	40
<b>9 Conclusions</b>	<b>41</b>
9.1 Future Work	42
<b>Bibliography</b>	<b>43</b>

# List of Figures

3.1	Overground Robotic Walker . . . . .	9
3.2	Linear Drive . . . . .	10
3.3	6-DOF load cell . . . . .	11
4.1	Sign Convention . . . . .	12
4.2	Walker Schematic . . . . .	13
4.3	ASOC Schematic . . . . .	13
4.4	Platform Schematic . . . . .	15
5.1	Velocity response of the walker. . . . .	17
5.2	Stiffness of Human-Walker interaction. . . . .	18
5.3	Human-Walker System block Diagram. . . . .	19
5.4	Bode plots for Admittance control with $J = 60\text{Kg}$ and $b = 60 \text{ Ns/m}$ . . . . .	22
6.1	Reference Velocity . . . . .	23
6.2	Measured Velocity . . . . .	23
6.3	Position Estimate . . . . .	25
6.4	Velocity Estimate . . . . .	25
6.5	Acceleration Estimate . . . . .	26
7.1	Force-Tunnel . . . . .	28
7.2	Damper based force tunnel . . . . .	29
7.3	Patient falling towards right. . . . .	31
7.4	Lateral trajectory of torso while walking . . . . .	32
7.5	COG lateral trajectory of a subject. . . . .	32
7.6	Transverse trajectory and SGC flag for detecting fall instance . . . . .	35
7.6	Transverse trajectory and SGC flag for detecting fall instance . . . . .	36
7.7	Spring-Damper system for Force-Tunnel . . . . .	37
8.1	Response time of supporting action. . . . .	39
8.2	Response time of supporting action. . . . .	40

*Dedicated to my hero, the missile man of India, Dr. A.P.J. Abdul Kalam*

# Chapter 1

## Introduction

Stroke is one of the leading causes of disability around the world and is the third most frequent cause of death worldwide [13]. Stroke is usually caused by the burst of blood vessels which lead to partial paralysis of one side of the body. This leads to disturbance in several daily activities like eating, walking and speaking.

Human gait is the most basic form of human locomotion and it is functional due to the intricate network between neuro-physiological network and the musculo-skeletal system. Stroke causes damage to this network causing many patients to lose their ability to walk [37] [28]. This often leads to abnormal gait patterns in stroke survivors like reduced gait speed, shortened step length gait instability and asymmetry[15] [26] and [6]. In addition to this loss of mobility, stroke severely affects the patient's moral and self-confidence due to the increased dependency on others.

The main purpose of gait therapy is to improve and restore the gait patterns through a proper gait rehabilitation regime. The focus of this regime is not only towards improving the ability to walk, but also for restoring the quality of walking. This ultimately leads to an enhanced quality of life.

Brain has an interesting property called brain plasticity which enables it to reconnect and reorganize neural pathways which were affected by the stroke. This is achieved by repetitive and persistent simulations in the form of various physical exercises[9] [20] and [29].

The conventional gait therapy is based on active joint mobilization of lower limbs, ankle, knee and the hip joint. This is often performed with the help of a therapist. The therapist facilitates pelvic motion to improve control and mobility of the patients. Studies have shown that such therapies can be extremely beneficial for the rehabilitation of stroke survivors [17] [10]. However, conventional rehabilitation is limited by the availability, duration and the frequency of training sessions primarily due to the excessive and exhaustive physical efforts required from therapists in rehabilitation therapies.A therapist is often required to lift up the body-weight of patients

which often causes back injuries to them. This in turn puts more burden on the existing health care systems. Also the rehabilitation sessions provided by different therapists are very subjective which can prove to be an obstacle when providing rehabilitation for longer times. Additionally, the cost of repetitive treatment for stroke patients may be very costly due to the increased number of stroke patients because of increased life expectancy and increasing elderly population while the supply of therapists is limited.

An interesting alternate to the conventional gait rehabilitation is robot assisted gait rehabilitation (RGAR). These devices have gained popularity due the possibility of automating gait therapy [19] [8] and [7]. These devices can allow more intensive and repetitive motions required in a gait therapy at reasonable costs and availability. Several studies indicate that such devices can be at least as effective as a human therapist [36].

Several types of Robotic Gait Rehabilitation devices (RGR) have been developed both in the academia and industry. These include treadmill based [32] [3] [12], foot-plate based [18] and the overground walker [27] [1] [16] [35]. Among all these designs rehabilitation by the overground walker has the biggest similarity to that of a human provided therapy as both of them involve actual walking on the ground [14]. The objective of an overground walker is to give body weight support to the patient while walking on the ground. This will relieve therapists of laborious work of supporting the patients and focus specifically on their gait training [4].

However there are several challenges to using overground robotic walkers. The biggest problem is of maintaining safety of operation. For example, falling is the most serious problems of the user and the fear of falling can increasing the anxiety levels in stroke penitents [34]. Additionally the walker needs to follow the user very intuitively without causing the user to loose his/her balance while walking[11]. The walker is also required to provide body weight support to the user to ease the rehabilitation therapy.

Thus it is important to have sufficient safety measures in the overground walker before they can be deployed for stroke rehabilitation. The objective of this thesis is to address the safety issues involved in the robotic walker. The problem statement of this thesis is defined in section 1.1 and the associated research challenges are mentioned in section 1.2. Finally sections 1.3 and 1.4 discuss the contributions made in this work and the structure of this thesis respectively.

## 1.1 Problem Statement and Research Challenges

This thesis addresses the problem of ensuring safety in overground robotic walker. Safety mechanisms are introduced by designing appropriate controllers. The overall control is divided into two categories as shown below:

- **Admittance control for intuitive use of walker.** The walker is expected to have an intuitive driving mechanism so as to minimize the mental efforts required by the user. Admittance control is used to drive the walker where force signals from the user are converted to velocity commands for the walker. It is desired that the admittance control be very ‘light’ which means that it should not have very high damping coefficients also to have good synchronization with the user it is important to have low mass parameter in the control. However decreasing the admittance parameters indefinitely is not the solution as it will make the robotic walker extremely unstable [24]. Instability in the walker is manifested in terms of undamped oscillations while under use. This can have serious consequences for the patient as the walker will be exerting excessive force on them. Thus, it is extremely important to have a safe admittance control which does not encourage undamped oscillations. Therefore, the challenge here is to come up with admittance control parameters which can guarantee stable walker operation while maintaining a ‘light’ and intuitive control behaviour.
- **Safety Control for fall prevention.** Apart from ensuring the safe and intuitive use of the walker it is important to provide sufficient safety to the user in the event of some gait instability. This support needs to be provided in both lateral and forward directions to bring the user to rest in minimum time and distance. The challenges to designing a safety control is multifaceted. Firstly it requires a reliable gait instability detection mechanism. This detection mechanism needs to have a high sensitivity and specificity. In other words, there should be a high rate of detection of gait instability and only a few cases of false positives. Another challenge in designing a safety control is to design effective support scheme which can effectively stabilize the user in limited time. The support scheme should not be too ‘stiff’ that it causes discomfort to the user neither should it be too ‘loose’ to be ineffective for fall prevention. Therefore the challenge lies in coming up with a reliable gait instability detection method and an effective support scheme.

## 1.2 Contributions

The main contributions of this thesis are in the form of ensuring stability of the overground walker. This is achieved in two separate yet inter-connected scenarios.

- Under regular walker use, an intuitive admittance control has been designed for the walker which guarantees a stable mode of operation. This is achieved by performing a through system identification of the walker to determine plant model. Then applying Routh's stability criterion to the closed loop transfer function to derive bounds on admittance control parameters that guarantee stability. Then tuning these parameters within the respective bounds to get best possible set of gain and phase margins. Efforts have been made to strike a balance between an intuitive driving and stable mode of operation.
- The novelty of this work is specially directed towards developing a safety control for the overground walker. The proposed safety control is composed of three major pieces. Firstly, an extremely accurate state estimation method is developed that make use of Kalman filter and a triple integrator as the system model for walker kinematics. Secondly, a fairly reliable mechanism to detect gait instability is proposed. The proposed mechanism exploits various unique features about human gait and provides a ‘Stable Gait Criterion’ (SGC) which is found to have high sensitivity and specificity. Strong mathematical proofs have been provided as a rational behind the SGC and experiments have been conducted to show its efficiency. Lastly, for an effective support scheme, ‘Force-Tunnel’ concept is proposed whereby the user experience a force-field around them which provides adequate support to regain gait stability. An attempt to implement another popular ‘safety-zone’ based safety control for overground walkers is made and it is shown that the proposed safety control method is much better than the earlier reported version.

### 1.3 Thesis Structure

**Chapter 1** first introduces the problems faced by current overground robotic walkers. Then the challenges involved in this problem were discussed followed by the contributions. The remaining Chapters are organized in the following way.

- Chapter 2 “**Related Works**” introduces the ideas of force control for robotic manipulation. It discusses the direct force control methods where the end-effector contact force is directly controlled. Indirect force control strategies when explicit force control is not possible and instead is used via motion control. This chapter also mentions a unique idea to do implicit force control of velocity controlled robots.
- Chapter 3 “**Robotic Walker**” introduces the overground robotic walker used in this work. It details about various components of the robotic walker along with their visuals.
- Chapter 4 “**Walker Kinematics**” elaborates the kinematic model of the overground robotic walker. It discuss the model of ASOC wheels and their relation to the platform and also the inverse kinematic model.
- Chapter 5 “**Admittance control of Walker**” thoroughly investigates the human-walker system model. It describes the walker velocity transfer function and the associated system identification to find the model parameters. This chapter also discuss the stability analysis for designing a safe admittance control for the walker.
- Chapter 6 “**State Estimation**” investigates the use of Kalman filters for use in state estimates. It describes the associated Kalman equations, parameters and its results.
- Chapter 7 “**Safety Control**” introduces the idea of force-tunnel for providing adequate support during fall instant. Two types of triggers for the safety control are discussed; one is based on a simple idea of using maximum deviation from the mean position. The second trigger is based on the concept of ‘Stable Gait Criterion’ (SGC) which is based on key properties of a human gait. A proof of the existence of SGC is also included. The chapter investigates the effectiveness of the SGC and provides elaborate explanation about the physical implementation of the force-tunnel.
- Chapter 8 “**Results**” discuss the performance of the safety control when tested on five subjects. The performance criteria were the response time and critical distance of the safety control.
- Chapter 9 “**Conclusions and Future Work**” This chapter contains the final remarks regarding the work done in this thesis. It also briefly discuss the scope for future work.

# Chapter 2

## Related Work

### 2.1 Force Control

Research in robot force control has grown rapidly in last thirty years [33] [31]. These developments have been motivated by the idea of providing robotic systems with enhanced sensory capabilities. These robots with force, touch, distance, and visual feedback are said to autonomously operate in unstructured environments apart from the usual industrial shop floor. From the developments in telemanipulation, the force feedback was thought to assist the human operators in the remote manipulation of objects with a slave manipulator. Currently, cooperative robot systems have been researched where two or more dexterous robots are able to coordinate to complete said tasks. Force control plays an important role in achieving robust and versatile behaviour of robotic systems in unstructured environments by providing intelligent responses to unforeseen situations and enhancing human-robot interaction.

Control of the physical interaction between a manipulator and its surroundings is crucial for the success of a number of practical tasks where the end-effector is required to manipulate an object or perform some activity on a surface. During contact, the work-space may set constraints on the geometric paths that can be followed by the end-effector. These constraints are referred to as *Kinematic constraints*. In other cases, the contact task is characterized by a dynamic interaction between the robot and its surroundings that can have inertial, dissipating and elastic properties. In such cases a pure kinematic based control activity is generally not successful. Accurate planning is not possible due to the high model uncertainties in the robot model parameters and details about the behaviour of the environment. In practice, these errors can lead to residual contact forces and moments which can cause deviation of the end-effector from the desired trajectories. Even with very detailed control algorithms this can lead to contact force saturation and the eventual breakage of joint actuators and other parts. Higher the environment stiffness, higher is the damage associated with such errors.

Active interaction control enables compliance in a manipulator by means of an appropriate control mechanisms. This requires the measurement of the contact force and moments which are used as a feedback to the controller and used to generate desired trajectories of end-effector in an online fashion. The active force control scheme is broadly classified into indirect and direct force control paradigms. This classification is based on the explicit closure of the force feedback loop. In the indirect case, force control is achieved by the means of motion control while in the case of the direct force control, explicit force loop exists.

### 2.1.1 Indirect Force Control

Impedance control or admittance control is the indirect method of implementing force control. In this method, deviation of the end-effector from reference trajectory is used as error signal for the control which outputs force signals. The relationship between the input position and output force is expressed in terms of inertial, damping and elastic parameters. Therefore, a robot manipulator under impedance or admittance control behaves like an equivalent mass-spring-damper system with variable parameters [25]. The impedance control differs from the admittance control in the way robot reacts to the environment. In impedance control, the position error results in a force signal whereas in admittance control a force error produces a position signal. In other words, impedance and admittance control can be said to be exact opposites of each others.

### 2.1.2 Direct Force Control

The direct force control methods utilizes the closure of force feedback signal to explicitly alter the contact force of the end-effector [38]. Direct force control is often referred to as *Hybrid Force/Motion Control* because it often implemented along with position control. This control method splits up simultaneous control of both end-effector motion and contact forces into two separate decoupled sub problems. The first problem is simply a position control problem which utilizes various common position control methods like PID. The second problem uses inverse robot dynamics to calculate the error between the reference and measured contact force signals. Direct force control is further divided into two separate groups viz; Explicit force control and implicit force control.

#### 2.1.2.1 Explicit Force control

Under direct force control, those cases where explicit dynamic model of the robot is known, explicit force control is possible [22]. In this method end-effector force is controlled by explicitly commanding joint torques by the controller. The contact force is also sensed using a force and moment sensor to calculate the force error.

### 2.1.2.2 Implicit Force control

Here the end-effector force is controlled by modifying the reference trajectory of an inner loop joint position/velocity controller[30]. The input to the controller is the sensed force error. This method relies on some model of interaction with the environment. This method is therefore limited in cases where either the inner control loop is poor or interaction model is non-linear.

## 2.2 Safety Control

Safety control in overground robotic walker has previously been discussed for the KineAssist robot. Here, the concept of a ‘Safety Zone’ was first introduced whereby a patient’s upper body range of motion was limited. The ‘Safety Zone’ is defined as the range of excursions of the trunk, detailed by a clinician, in which the user can move without any assistance or hindrance from the device. The safety control is enabled at the boundary of this range and the trunk support provided in the KineAssist implements a compliant constraint. The compliant constraint is adjustable in position and stiffness which allows catching the patient when he or she loses balance.

# Chapter 3

## Robotic Walker

Several robotic platforms have been proposed in the literature for rehabilitation of stroke patients. However as reported in several studies, it is important to have the overground walking platform for proper sensory input and feedback to rehabilitate the appropriate sensory feedback. It is also essential for the device to provide multi-plane movements comprising forward-backward as well as lateral and rotational mobility with any hindrance. Additionally, the six DOFs of pelvic motion needs to be supported during the gait training. In the view of these key features, an overground robotic walker shown in figure 3.1 is designed whose structure is explained in the following chapter.

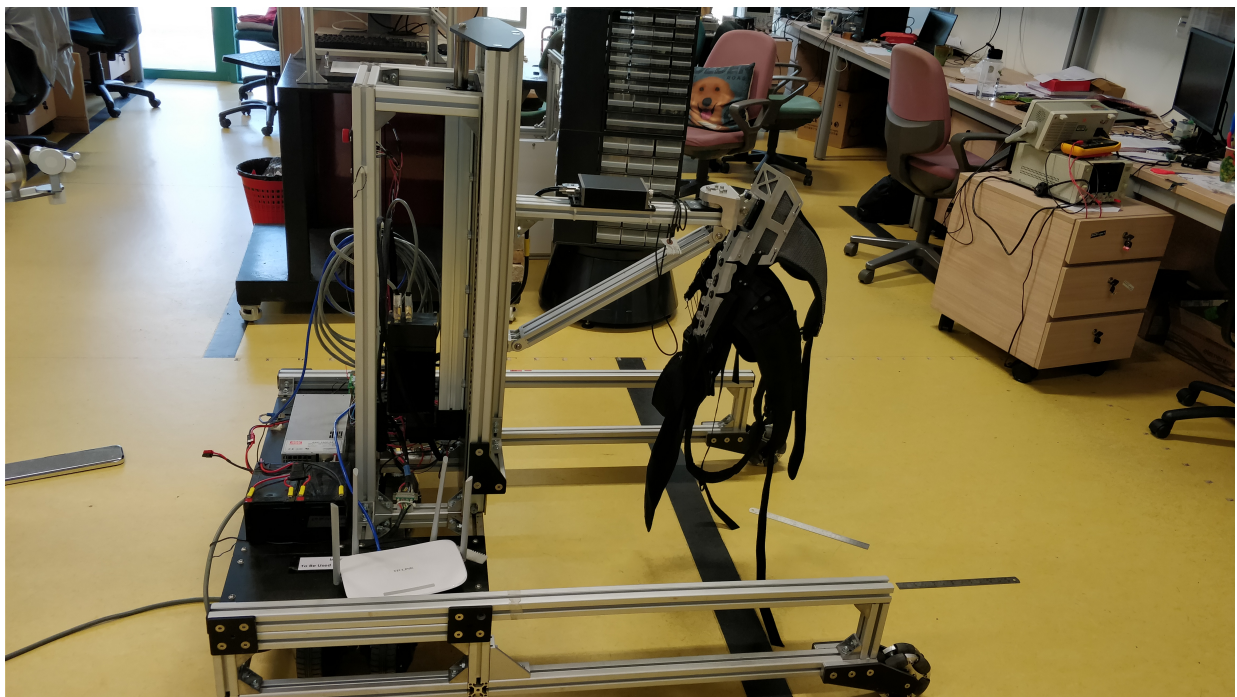


FIGURE 3.1: Overground Robotic Walker

### 3.1 Omni-Directional Platform

The walker is primarily composed of an omni-directional platform as shown in figure 3.1. The platform provides completely holonomic mobility on the ground. The platform is actuated by a pair of Active Split Offset Castors (ASOCs). Each ASOC consist of two motor actuated wheels that can rotate independently.

### 3.2 Linear Drive

The Linear drive is used to provide force control in the vertical direction. This is required to provide ‘Body Weight Support’ (BWS) to the stroke patient to facilitate their gait rehabilitation. The BWS unit of the overground walker is shown in figure 3.2.

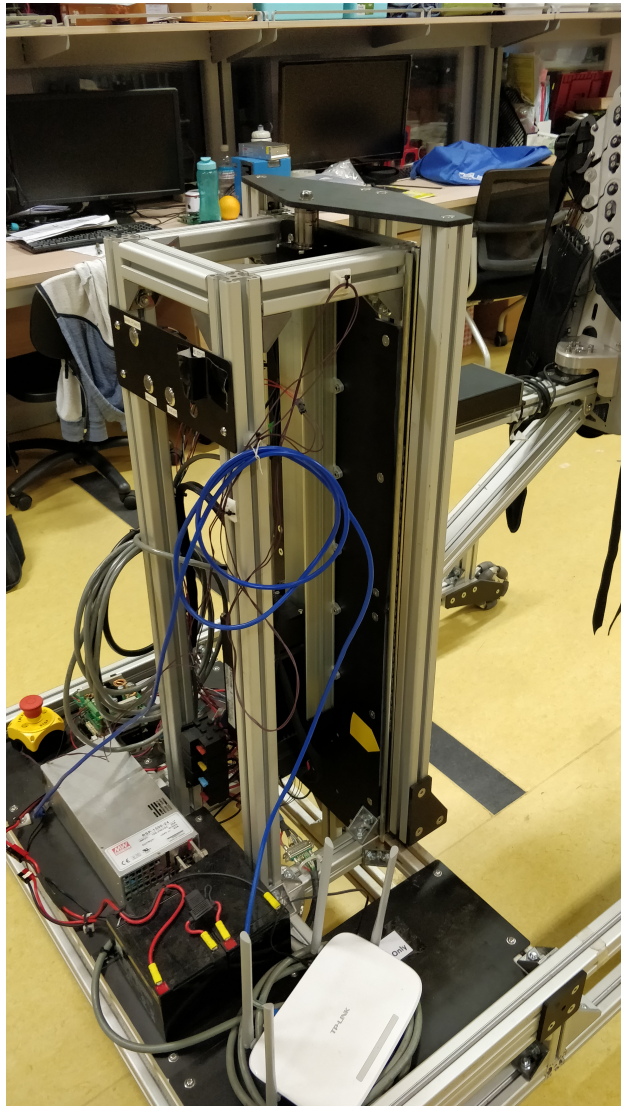


FIGURE 3.2: Linear Drive

### 3.3 Sensors.

The overground walker is fitted with several sensors for effective control operations.

- There are two pairs of encodes (total four) in the two ASOCs of the omni-directional platform. These provides accurate ( $\pm 1\text{cm}$ ) position information about the wheels.
- The linear drive is also fitted with an encoder having an accuracy of ( $\pm 1\text{mm}$ ).
- The walker is also fitted with a 6-axis Force/Torque load cell as shown in figure 3.3. The force readings are accurate upto  $1\text{N}$  and Torque reading are accurate upto  $.1\text{Nm}$ .



FIGURE 3.3: 6-DOF load cell

# Chapter 4

## Walker Kinematics

### 4.1 Sign Convention

The sign convention used in this thesis is shown in figure 4.1. The Y-axis is often referred to as the lateral direction. The X-axis is also referred to as the forward direction in this work. Please note that the coordinate system used in this work is a left-handed coordinate system. The direction of positive force signals correspond to the positive directions of walker position.

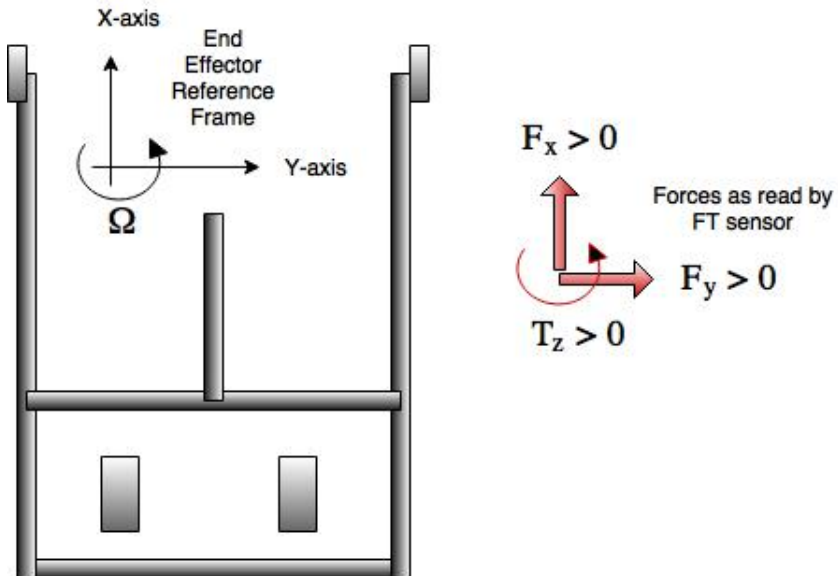


FIGURE 4.1: Sign Convention

## 4.2 Wheel Kinematics

Figure 4.2 shows the schematic of walker. The wheel velocities ( $v_{ll}, v_{lr}, v_{rl}, v_{rr}$ ) are manipulated to obtain desired end-effector velocities i.e. ( $V_{px}, V_{py}, \Omega$ ). The kinematic relation between the wheel velocities and end-effector velocities is based on the angular values of  $\alpha_1$  and  $\alpha_2$ .

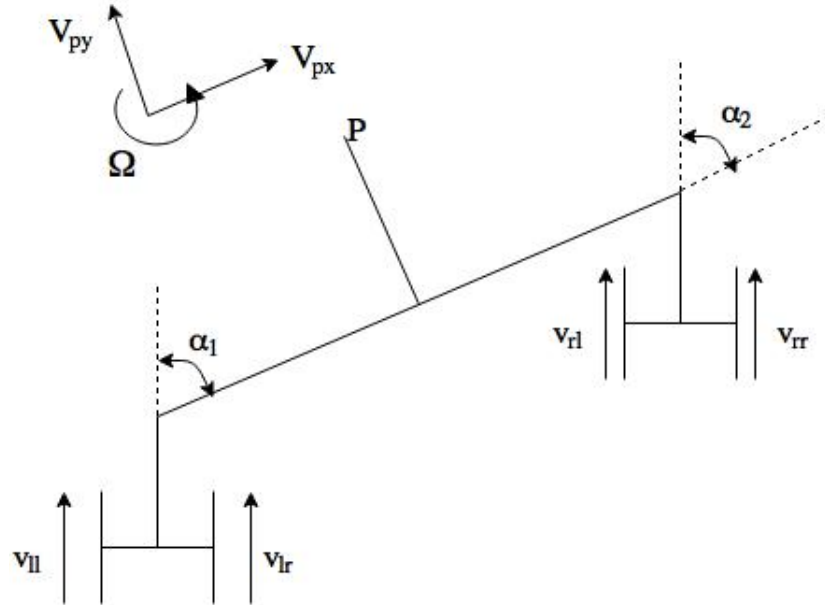


FIGURE 4.2: Walker Schematic

In order to develop inverse kinematics of the walker consider a single ASOC as shown in figure 4.3.

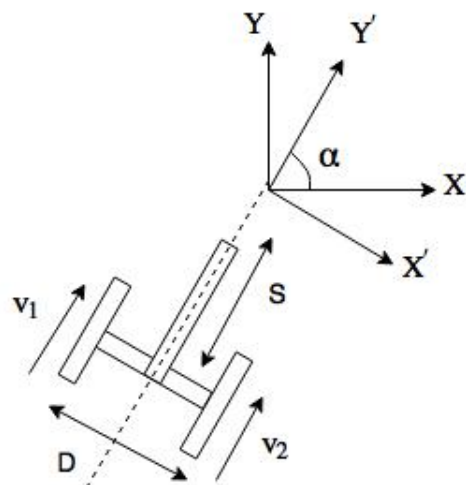


FIGURE 4.3: ASOC Schematic

Let  $u = [v_1 \ v_2]^T$  and  $q_w = [v_{X'} \ v_{Y'}]$ . Then we have  $q_w = J_w u$ . Where,

$$J_w = \begin{bmatrix} S/D & -S/D \\ 1/2 & 1/2 \end{bmatrix} \quad (4.1)$$

Additionally, for  $q = [v_X \ v_Y]$ , we have  $q = R(\alpha)q_w$ . Where the rotation matrix  $R(\alpha)$  is expressed as

$$R(\alpha) = \begin{bmatrix} \cos(\alpha) & -\sin(\alpha) \\ \sin(\alpha) & \cos(\alpha) \end{bmatrix} \quad (4.2)$$

$$\implies q = R(\alpha)J_w u \quad (4.3)$$

The inverse equation is

$$u = J_w^{-1}R^{-1}(\alpha)q \quad (4.4)$$

Therefore, for the two ASOCs we have the following relations.

$$\begin{bmatrix} v_{ll} \\ v_{lr} \\ v_{rl} \\ v_{rr} \end{bmatrix} = \begin{bmatrix} \cos(\alpha_1) + \sin(\alpha_1) & \sin(\alpha_1) - \cos(\alpha_1) \\ \cos(\alpha_1) - \sin(\alpha_1) & \sin(\alpha_1) + \cos(\alpha_1) \\ \cos(\alpha_2) + \sin(\alpha_2) & \sin(\alpha_2) - \cos(\alpha_2) \\ \cos(\alpha_2) - \sin(\alpha_2) & \sin(\alpha_2) + \cos(\alpha_2) \end{bmatrix} \begin{bmatrix} v_{x1} \\ v_{y1} \\ v_{x2} \\ v_{y2} \end{bmatrix} \quad (4.5)$$

### 4.3 Platform Kinematics

From figure 4.4 we arrive at the following relation between end-effector velocities and velocities of the two ASOCs.

$$\begin{bmatrix} v_{x1} \\ v_{y1} \\ v_{x2} \\ v_{y2} \end{bmatrix} = \begin{bmatrix} 1 & 0 & l' \sin(\theta) \\ 0 & 1 & -l' \cos(\theta) \\ 1 & 0 & l' \sin(\theta) \\ 0 & 1 & l' \cos(\theta) \end{bmatrix} \begin{bmatrix} v_{px} \\ v_{py} \\ \Omega \end{bmatrix} \quad (4.6)$$

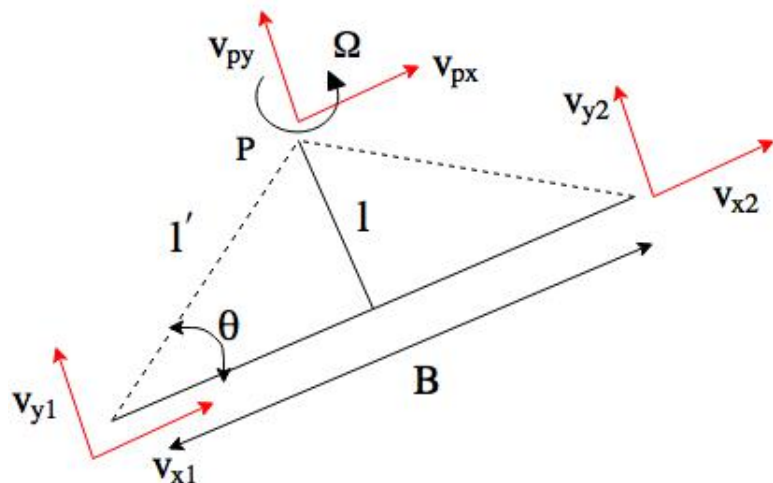


FIGURE 4.4: Platform Schematic

## Chapter 5

# Admittance Control of Walker

The walker is required to follow the user intuitively without requiring a lot of efforts by the user. In the current overground walker, a 6-axis force/torque load cell is provided to sense the contact force between the user and the walker. This force signal is used as a feedback for the force control. Several force control strategies have been discussed in Chapter 2. However, given the walker structure detailed in Chapter 3 several of those techniques cannot be applied. Since the amount of current provided in the omni-directional platform motors cannot be altered by an external control loop, it is difficult to do direct force control. Even implicit force control methods is not possible due to the unavailability of interaction dynamics. Thus, for the current robotic walker, admittance control is used where based on the force error, the controller outputs velocity commands for the wheels.

A typical admittance control equation has a dynamic relation between force error  $f(t)$  and the robot's position  $\theta(t)$  as shown below.

$$f(t) = M(t)\ddot{\theta}(t) + b(t)\dot{\theta}(t) + K(t)\theta(t) \quad (5.1)$$

In frequency domain, for fixed parameters we have the admittance value  $Y(s)$  as:

$$Y(s) = \frac{\Theta(s)}{F(s)} = \frac{1}{Ms^2 + bs + K} \quad (5.2)$$

The mass  $M(t)$  represents the inertia of the system. System damping  $b(t)$  and stiffness  $K(t)$  are used for energy dissipation and storage. The admittance parameters can be altered to generate different system behaviours. It is extremely important to have right set of values for mass, damper and spring otherwise it may lead to system instability. The implementation of admittance control for the overground robotic walker is explained in the subsequent sections.

## 5.1 Walker Velocity Transfer function.

When velocity commands are sent to the platform wheels, they take a finite amount of time to achieve the reference velocity. The velocity response of the platform is modeled as a second order system. A typical second order system transfer function is as follows:

$$H(s) = \frac{V_m(s)}{V_r(s)} = \frac{\omega_n^2}{s^2 + 2\zeta\omega_n s + \omega_n^2} \quad (5.3)$$

Here the  $V_r$  is the commanded reference velocity and  $V_m$  is the measured walker velocity. The natural frequency of this second order system is denoted by  $\omega_n$  and the damping coefficient is represented by  $\zeta$ .

To find the values of natural frequency and damping coefficient, we perform system identification of the walker. This is done by giving a step reference velocity command to the walker and measuring the wheel transient response as shown in figure 5.1. The red line denotes the reference velocity  $V_r(t)$  stepped at time  $t = 2s$ . The blue line refers to the raw velocity measurement  $V_m(t)$ .

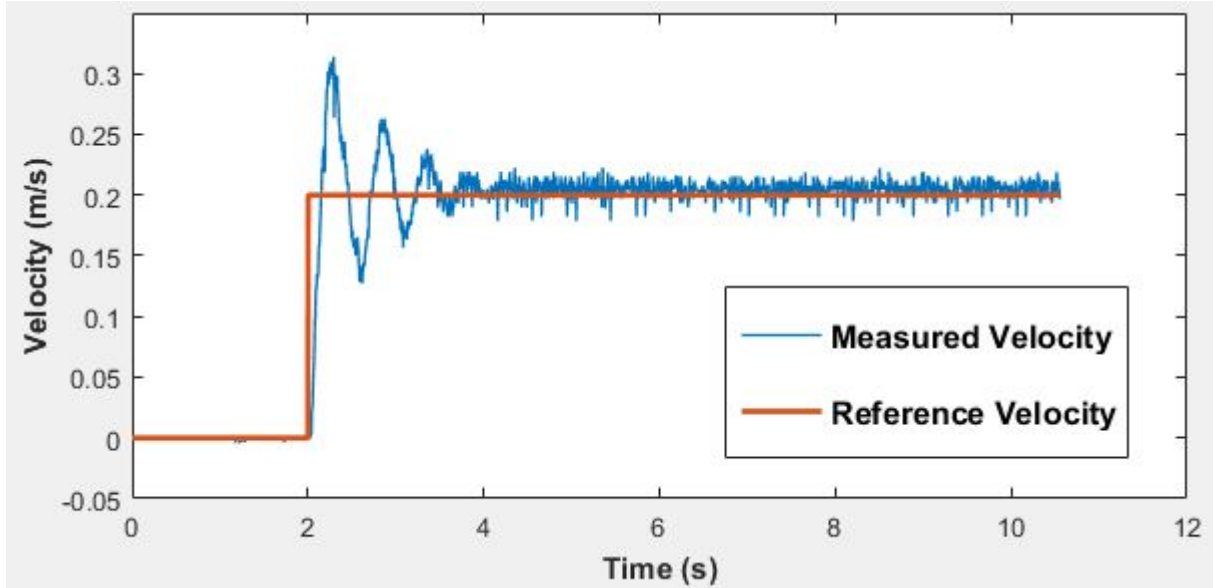


FIGURE 5.1: Velocity response of the walker.

By calculating the time between consequent trough and crest ( $\hat{T}$ ) and the value of the peak overshoot ( $M_p$ ) we can derive the natural frequency and damping coefficients by using the following relations.

$$\hat{T} = \frac{\pi}{\sqrt{1 - \zeta^2}\omega_n} \quad (5.4)$$

and,

$$M_p = \frac{y_{max} - y_{ss}}{y_{ss}} = \exp \left[ \frac{-\pi\zeta}{\sqrt{1 - \zeta^2}} \right] \quad (5.5)$$

Where  $y_{max}$  and  $y_{ss}$  refer to the peak overshoot and steady state velocities respectively. From figure 5.1 we can note that  $\hat{T} \approx 0.3s$ . Since  $y_{max} \approx 0.314m/s$  and  $y_{ss} = 0.2m/s$ , we obtain  $M_p \approx 0.57$ . Thus, from equations 5.4 and 5.5 we obtain  $\zeta = 0.17$  and  $\omega_n = 10.64rad/s$ . Therefore, the velocity transfer function of the walker is found to be

$$H(s) = \frac{V_m(s)}{V_r(s)} = \frac{113.20}{s^2 + 3.62s + 113.20} \quad (5.6)$$

## 5.2 Human-Walker interaction model

The physical interaction between the user and the walker is modelled as a mass and a damper system with stiffness  $K$  and damping coefficient  $b$  respectively. The stiffness value is calculated by measuring the slope of the best fit line as shown in figure 5.2. Here the magnitude of contact force was measured for five compression values. The slope of the best fit line is calculated as around  $150N/m$ . Thus we arrive at the stiffness coefficient  $K = 150N/m$ . From several studies on human muscle [2], the damping factor is found to be roughly one-tenth of the stiffness value. However, for the ease of analysis, we assume the damping coefficient to be equal to zero.

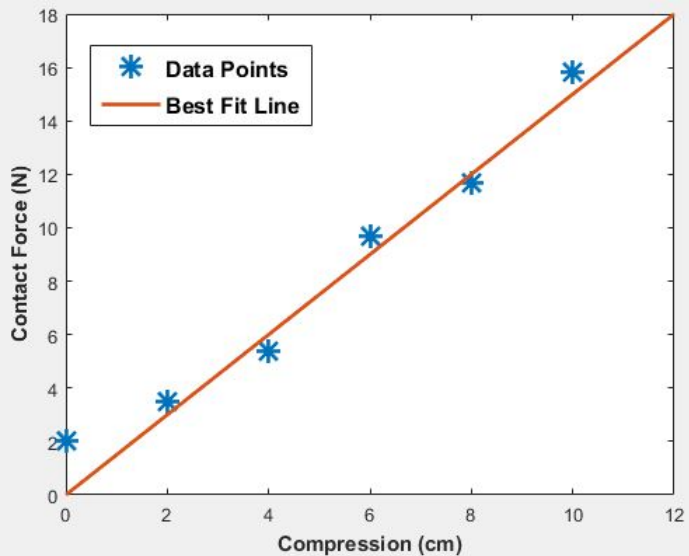


FIGURE 5.2: Stiffness of Human-Walker interaction.

### 5.3 Human-Walker System block diagram.

From the discussions in previous sections we can finally arrive the closed loop system block diagram as shown in figure 5.3. Here  $x_{patient}$  is the reference position of the patient.  $x_{walker}$  denotes the position of the walker. Based on the human-walker interaction model discussed in the previous section the difference between  $x_{patient}$  and  $x_{walker}$  gives rise to a contact force  $F_{sensed}$ . The admittance control consists of only the inertia term  $J$  and damping  $b$ . The admittance control outputs the reference velocity  $\hat{v}_w$  to the wheels which in turn leads to the actual walker velocity  $v_w$  by following a second order system model as discussed in section 5.1. The integral of actual walker velocity is used to arrive at the walker position.

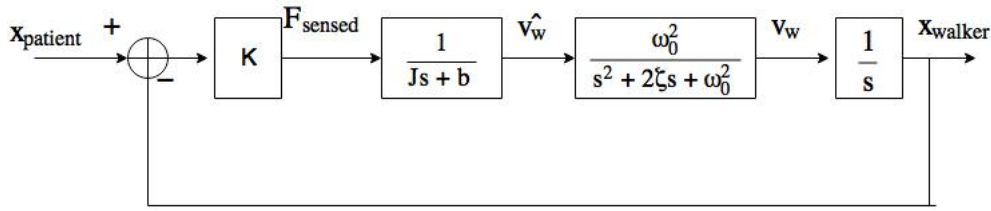


FIGURE 5.3: Human-Walker System block Diagram.

It is essential to note that the interaction stiffness and velocity tracking is fixed for the human-robot system. By altering the inertia and damping values of the admittance control, the walker can be made ‘light’ to use and its motion can be made in sync with the periodic motion of the patient. Choosing high values for inertia and damping will make the walker ‘heavy’ and its motion will be out of phase to that of patient on the contrary, choosing small values of inertia and damping can lead to undamped oscillation of the human-walker system. Therefore it is important to choose the parameter values which insure system stability. The subsequent section deals with the stability analysis of the overall system thus deriving adequate bounds on admittance parameters.

### 5.4 Stability Analysis of Human-Walker system.

The open loop transfer function of the human-walker system is as follows,

$$G(s) = \frac{K\omega_n^2}{Js^4 + (2J\zeta\omega_n + b)s^3 + (\omega_n^2 J + 2\zeta\omega_n b)s^2 + b\omega_n^2 s} \quad (5.7)$$

The closed loop transfer function is therefore calculated as

$$H(s) = \frac{K\omega_n^2}{Js^4 + (2J\zeta\omega_n + b)s^3 + (\omega_n^2 J + 2\zeta\omega_n b)s^2 + b\omega_n^2 s + K\omega_n^2} \quad (5.8)$$

In order to determine the stability of the above closed loop system Routh's stability criteria is employed. The characteristic equation for the given system is as follows.

$$Js^4 + (2J\zeta\omega_n + b)s^3 + (\omega_n^2 J + 2\zeta\omega_n b)s^2 + b\omega_n^2 s + K\omega_n^2 = 0 \quad (5.9)$$

The corresponding Routh's table is as shown in below table.

$s^4$	J	$\omega_n^2 J + 2\zeta\omega_n b$	$K\omega_n^2$
$s^3$	$2J\zeta\omega_n + b$	$b\omega_n^2$	0
$s^2$	$\Delta_1$	$K\omega_n^2$	0
$s^1$	$\Delta_2$	0	0
$s^0$	$K\omega_n^2$	0	0

Where for the system stability, the following constraints need to be satisfied.

$$\Delta_1 = \frac{(2J\zeta\omega_n + b)(\omega_n^2 J + 2\zeta\omega_n b) - Jb\omega_n^2}{2J\zeta\omega_n + b} > 0 \quad (5.10)$$

$$\Delta_2 = \frac{[(2J\zeta\omega_n + b)(\omega_n^2 J + 2\zeta\omega_n b) - Jb\omega_n^2][b\omega_n^2] - (2J\zeta\omega_n + b)^2(K\omega_n^2)}{(2J\zeta\omega_n + b)(\omega_n^2 J + 2\zeta\omega_n b) - Jb\omega_n^2} > 0 \quad (5.11)$$

Firstly eq. 5.10 can be rewritten in the following form.

$$(2J\zeta\omega_n + b)(\omega_n^2 J + 2\zeta\omega_n b) > Jb\omega_n^2 \quad (5.12)$$

$$\implies 2\zeta J^2\omega_n^3 + 4\zeta^2\omega_n^2 bJ + 2\zeta\omega_n b^2 > 0 \quad (5.13)$$

which is trivially true. Therefore the constraint  $\Delta_1 > 0$  is always satisfied.

Now for the constraint  $\Delta_2 > 0$  we can write eq 5.11 as follows.

$$2\zeta J^2\omega_n^3 + 4\zeta^2\omega_n^2 bJ + 2\zeta\omega_n b^2 > (2J\zeta\omega_n + b)^2 \frac{K}{b} \quad (5.14)$$

Now dividing the above equation by  $J^2$  we have

$$\implies 2\zeta\omega_n(\frac{b}{J})^2 + 4\zeta^2\omega_n^2(\frac{b}{J}) + 2\zeta\omega_n^3 > (2\zeta\omega_n + \frac{b}{J})^2 \frac{K}{b} \quad (5.15)$$

Now let  $\frac{b}{J} = x$ ,  $b^{-1} = y$  and  $2\zeta\omega_n = \alpha$ . We arrive at

$$\implies \alpha x^2 + \alpha^2 x + \alpha\omega_n^2 > (\alpha + x)^2 Ky \quad (5.16)$$

$$\implies (\alpha - Ky)x^2 + (\alpha^2 - 2\alpha Ky)x + (\alpha\omega_n^2 - \alpha^2 Ky) > 0 \quad (5.17)$$

The above equation can be treated as a quadratic inequality in the variable  $x$ . Therefore, in order for the above inequality to be true the determinant of the above quadratic in  $x$  must negative along with the constraint  $\alpha - Ky > 0$ . Therefore for  $D(x) < 0$  we get

$$(\alpha^2 - 2\alpha Ky)^2 - 4(\alpha - Ky)(\alpha\omega_n^2 - \alpha^2 Ky) < 0 \quad (5.18)$$

$$\implies 4K\alpha\omega_n^2 y + (\alpha^4 - 4\alpha^2\omega^2) < 0 \quad (5.19)$$

$$\implies y < \frac{4\alpha\omega_n^2 - \alpha^3}{4K\omega_n^2} \quad (5.20)$$

Also from the prior discussion on  $D(x) < 0$  we have

$$y < \frac{\alpha}{K} \quad (5.21)$$

The equations 5.20 and 5.21 leads to the following bound on  $y$

$$y < \text{Min}\left[\frac{\alpha}{K}, \frac{4\alpha\omega_n^2 - \alpha^3}{4K\omega_n^2}\right] \quad (5.22)$$

Thus, in terms of admittance parameters  $J$  and  $b$  we have the following bounds for a stable human-walker system.

$$b > \text{Max}\left[\frac{K}{\alpha}, \frac{4K\omega_n^2}{4\alpha\omega_n^2 - \alpha^3}\right] \quad \forall \frac{b}{J} \in \mathbb{R} \quad (5.23)$$

Substituting the values of  $K$ ,  $\zeta$  and  $\omega_n$  we get  $b > 43Ns/m$  for stability of the system. However, it is also important to have good stability margins margins to account for the unmodelled factors.

For a good stability margin, admittance parameters values chosen were  $b = 60Ns/m$  and  $J = 60Kg$ . The corresponding bode plot of the human-walker system is shown in the figure 5.4. Sufficient gain margin of 18.1dB and phase margin of  $32^\circ$  were obtained.

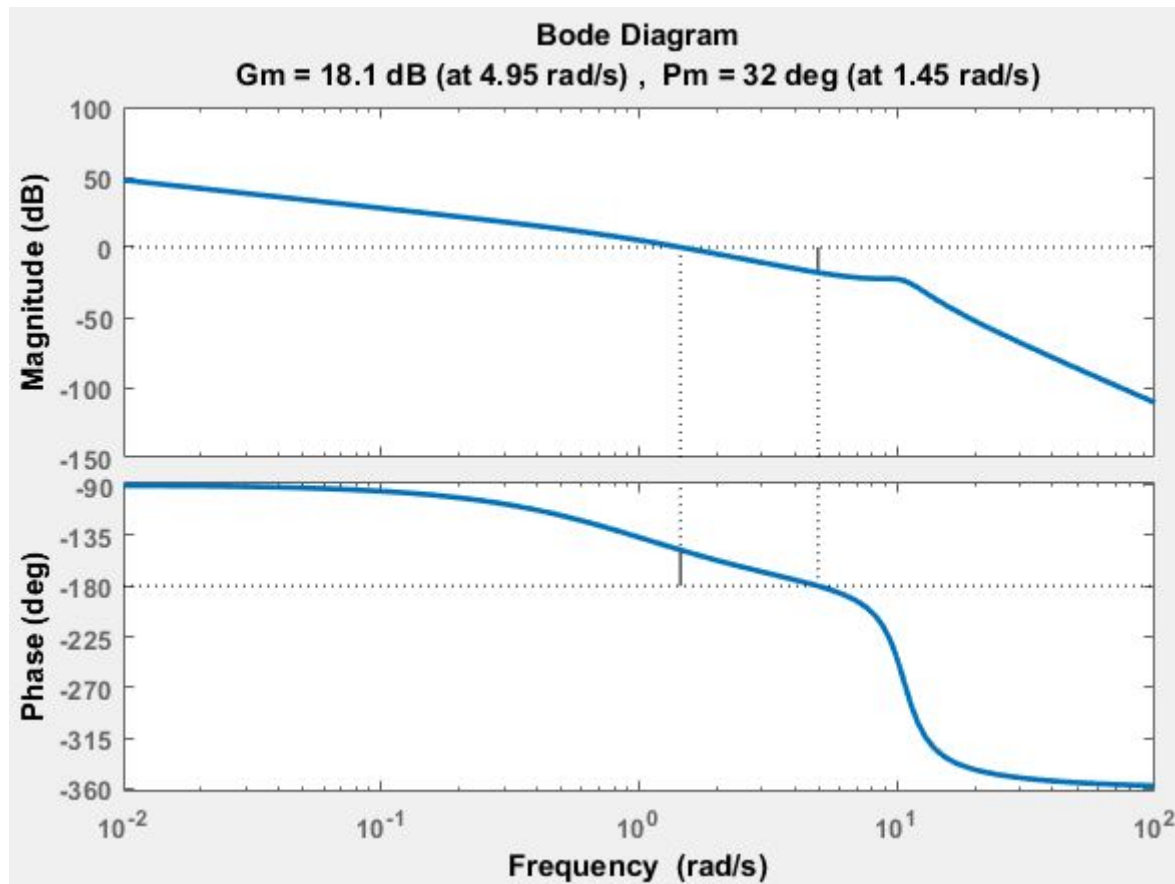


FIGURE 5.4: Bode plots for Admittance control with  $J = 60Kg$  and  $b = 60 \text{ Ns/m}$

# Chapter 6

## State Estimation

### 6.1 State Estimation: Kalman Filter

To deploy a reliable safety control, it is important to have an accurate estimate of walker states. The position estimates provided by walker's encoders are noisy. Subsequently their derivatives to obtain velocity and acceleration estimates are even more noisy. Figure 6.2 shows the measured velocity of the walker when given a sinusoidal reference velocity of frequency  $0.1\text{Hz}$  as shown in figure 6.1. Clearly it is difficult to use measured velocity signal for control.

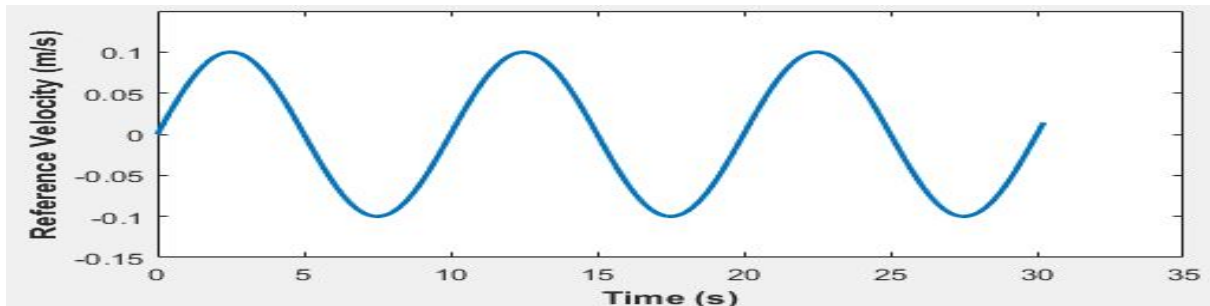


FIGURE 6.1: Reference Velocity

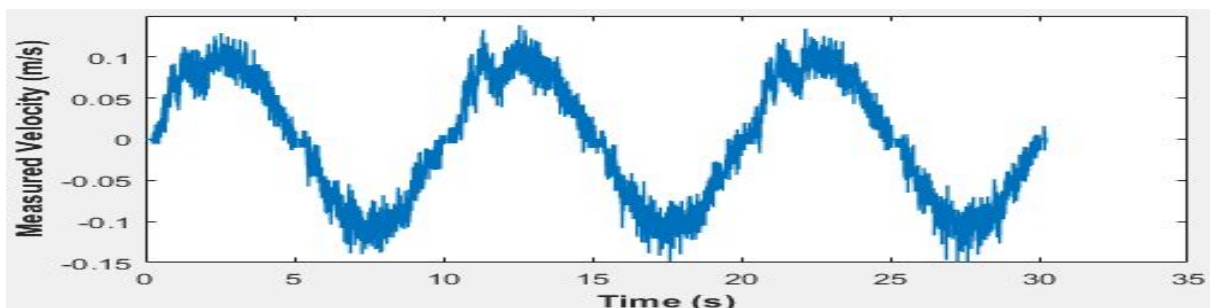


FIGURE 6.2: Measured Velocity

Kalman filter helps fuse the measured estimates with the model information to come up with optimal state estimates. Additionally, it also provides very low noise estimates of derivatives of position estimates like velocity and acceleration. The state vector of walker for both forward and lateral directions has the following form.

$$X_k = \begin{bmatrix} p_k \\ v_k \\ a_k \end{bmatrix} \quad (6.1)$$

The kinematic model of walker to estimate position, velocity and acceleration is called a ‘triple integrator’ and is mentioned as follows for discrete systems.

$$X_k = F_k X_{k-1} + G_k J_k \quad (6.2)$$

Here,  $F_k$  is called prediction matrix and  $G_k$  is the control matrix.  $J_k$  is the Jerk in position command to the walker. Their matrix forms are written as follows.

$$\begin{bmatrix} p_k \\ v_k \\ a_k \end{bmatrix} = \begin{bmatrix} 1 & dt & \frac{dt^2}{2} \\ 0 & 1 & dt \\ 0 & 0 & 1 \end{bmatrix} \begin{bmatrix} p_{k-1} \\ v_{k-1} \\ a_{k-1} \end{bmatrix} + \begin{bmatrix} 0 \\ \frac{dt^2}{2} \\ dt \end{bmatrix} J_k \quad (6.3)$$

The prediction equations used in Kalman filter are as per the following.

$$\hat{X}_k = F_k X_{k-1} + G_k J_k \quad (6.4)$$

$$\hat{P}_k = F_k P_{k-1} F_k^T + Q_d \quad (6.5)$$

Here  $X_{k-1}$  is the corrected state estimate for  $k - 1$  step and  $\hat{X}_k$  is the predicted state for step  $k$ .  $P_{k-1}$  is the corrected co-variance matrix for  $k - 1$  step and  $\hat{P}_k$  is the co-variance matrix for step  $k$ . Here  $Q_d$  is the process noise which was found to be.

$$Q_d = \begin{bmatrix} .1 & 0 & 0 \\ 0 & .1 & 0 \\ 0 & 0 & .1 \end{bmatrix} \quad (6.6)$$

The Kalman Gain  $K_k$  is calculated using  $H_k = [1 \ 0 \ 0]$  and measurement noise  $R_d = .01$ .

$$K_k = \hat{P}_k H_k^T (H_k \hat{P}_k H_k^T + R_d)^{-1} \quad (6.7)$$

The correction equations are mentioned as follows with  $Z_k$  being the measurement at step  $k$ .

$$X_k = \hat{X}_k + K_k(Z_k - H_k\hat{X}_k) \quad (6.8)$$

$$P_k = \hat{P}_k - K_k H_k \hat{P}_k \quad (6.9)$$

Using the above Kalman equations we arrive at better state estimates of walker. Figure 6.3 shows the position estimate of the walker when given a sinusoidal reference signal as shown in figure 6.1.

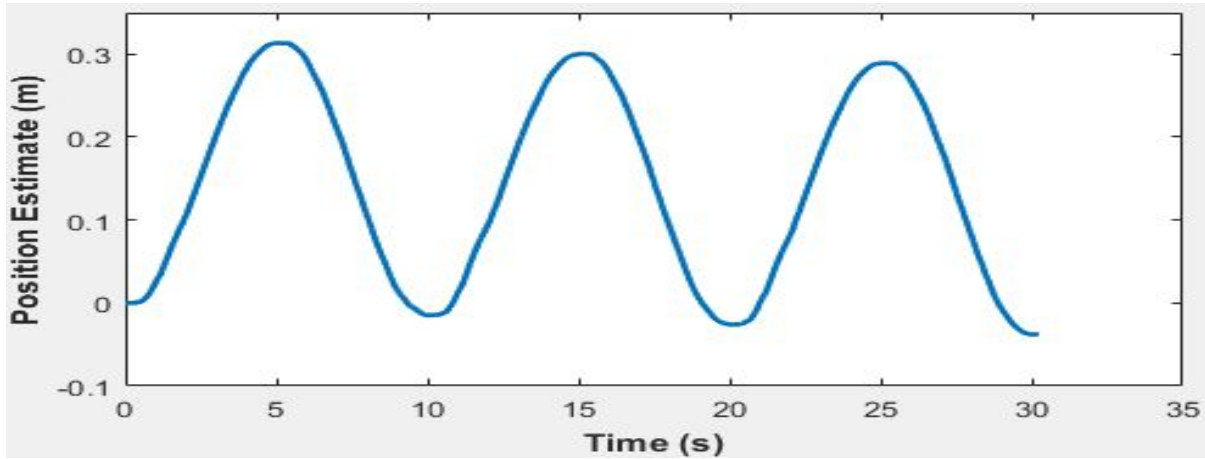


FIGURE 6.3: Position Estimate

The velocity estimate shown in figure 6.4 is far less noisy than the measured velocity signal in figure 6.2.

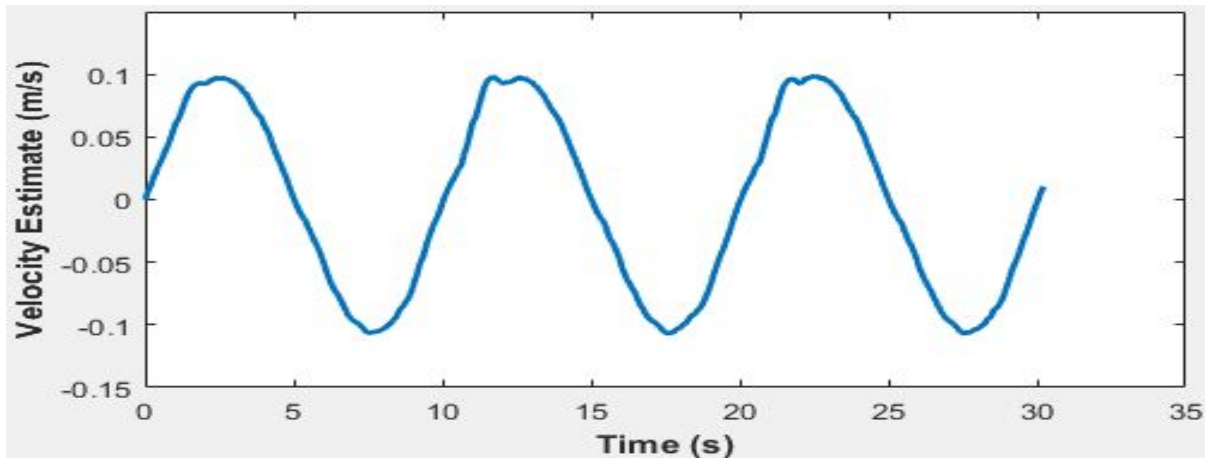


FIGURE 6.4: Velocity Estimate

Even the acceleration estimate shown in figure 6.5 is very smooth and can be used to develop safety control.

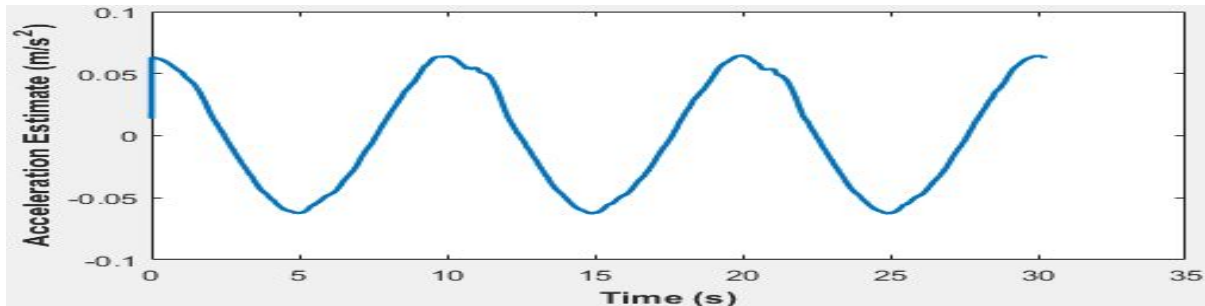


FIGURE 6.5: Acceleration Estimate

Thus the Kalman filter prove to be very effective in providing noise free estimates of walker position, velocity and acceleration. The position and acceleration estimates are used by Safety control to accurately detect gait instability and provide adequate supporting force.

# Chapter 7

## Safety Control of Walker

The overground robotics walker is tasked to follow the user and also provide required body weight support. Since the walker is in contact with the patient, it is extremely important to ensure safety of the user while working with the walker. For safety under normal walking conditions, safety is ensured by guaranteeing human-walker system stability which has already been discussed in the previous chapter on admittance control. This chapter deals with the special case of fall prevention by introducing a separate safety control. The concept of the safety control is based on the proposed concept called ‘Force-Tunnel’. It is essentially a mechanism to give adequate support to the user for restoring gait stability. Section 7.1 elaborates on the theoretical ideas about the force-tunnel. Section 7.2 implements the force tunnel using a very simple distance based triggering mechanism also called ‘safety-zone’ criteria. Section 7.4 proposes a completely novel triggering mechanism based on ‘Stable Gait Criterion (SGC)’ for enabling the force tunnel.

### 7.1 Force Tunnel

While walking there maybe instances when the user looses balance. In such cases the walker is required to provide support to the user just like any human therapist. The regular admittance control of the walker is insufficient to provide support during a falling instance. Therefore there is a need to develop an adequate supporting mechanism which can be implemented as a separate control loop.

The Force-Tunnel is used to provide support to the user when gait imbalance occurs. A typical force-tunnel is shown in figure 7.1. A force tunnel provides support  $F_{support}$  in both lateral as well as forward direction for fall prevention. A force tunnel is enabled using a criterion which can efficiently detect user’s gait instability. In this work such a criterion is denoted by the

function  $g(t)$ . Depending upon this criterion, the force tunnel can be divided into two regions as shown in figure 7.1. A supporting force is provided during unstable gait, denoted by  $(g(t) > \delta)$ , and is turned off during stable gait i.e.  $(g(t) \leq \delta)$ . Here  $\delta \in \mathbb{R}$  is used as the separating boundary between the two regions.

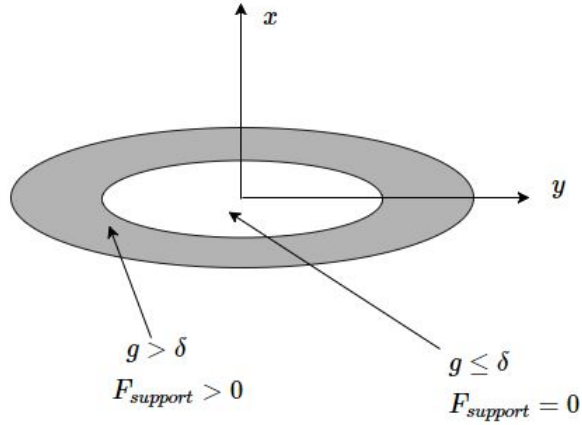


FIGURE 7.1: Force-Tunnel

## 7.2 Safety-Zone Criterion

Under the safety zone criterion, a displacement based criterion is used which is defined as follows:

$$g(t) = |Y(t)| \leq Y_1, Y_{-1} \quad (7.1)$$

Where,  $Y(t)$  is the current lateral displacement of the walker and  $\delta = Y_1, Y_{-1}$  represent the maximum possible displacements on the either side of the zero displacement point.

The force-tunnel is implemented using dampers on either side of the walker in the lateral direction as shown in figure 7.2.

Here  $M_0$  and  $b_0$  are the lateral admittance control parameters in the absence of force-tunnel.  $K$  is the spring constant of the damper,  $b_-$  and  $b_+$  are the damping coefficients for the left and right dampers respectively. Range of motion  $Y_{-1} < Y < Y_1$  is the ‘free-zone’ where the walker’s motion is not affected by the adjacent dampers. For  $Y < Y_{-1}$  and  $Y > Y_1$  the dampers are activated to provide lateral support.  $Y_{-2}$  and  $Y_2$  represent the maximum possible sideways deviation of walker. The control scheme for the above implementation is as follows.

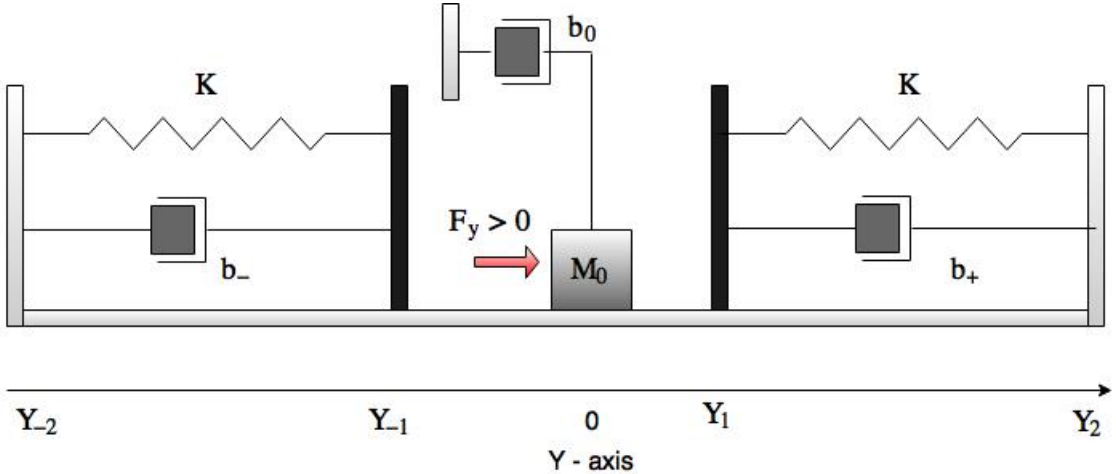


FIGURE 7.2: Damper based force tunnel

### 7.2.1 Control Scheme for Safety Zone

The dynamic equations to be followed by the walker are piece-wise defined for the regions  $Y_{-2} < Y < Y_{-1}$ ,  $Y_{-1} < Y < Y_1$  and  $Y_1 < Y < Y_2$ .

For  $Y_{-1} < Y < Y_1$ :

$$M_0 \ddot{Y} + b_0 \dot{Y} = F_y \quad (7.2)$$

For  $Y_{-2} < Y < Y_{-1}$ :

$$M_0 \ddot{Y} + b_0 \dot{Y} = F_y - b_- \dot{Y} - K(Y - Y_{-1}) \quad (7.3)$$

For  $Y_1 < Y < Y_2$ :

$$M_0 \ddot{Y} + b_0 \dot{Y} = F_y - b_+ \dot{Y} - K(Y - Y_1) \quad (7.4)$$

Eq. (1), (2) and (3) can together be expressed as

$$M_0 \ddot{Y} + b_0 \dot{Y} = F_y - \alpha(Y) \quad (7.5)$$

where,

$$\alpha(Y) = \begin{cases} b_- \dot{Y} + K(Y - Y_{-1}) & Y_{-2} < Y < Y_{-1} \\ 0 & Y_{-1} < Y < Y_1 \\ b_+ \dot{Y} + K(Y - Y_1) & Y_1 < Y < Y_2 \end{cases} \quad (7.6)$$

To make it easy for the patient to escape the damping region, when he/she is trying to return to the mean position, the damping coefficients of the two dampers are made zero. Therefore, we define  $b_-$  and  $b_+$  as

$$b_- = b\left(\frac{1 - sgn(\dot{Y})}{2}\right) \quad (7.7)$$

$$b_+ = b\left(\frac{1 + sgn(\dot{Y})}{2}\right) \quad (7.8)$$

where  $sgn()$  is the sign function.

### 7.2.1.1 Calculation of parameters

The parameter value are based on the following constraints.

- Maximum lateral force provided by the walker ( $F_{ymax}$ ).
- Maximum allowable damping range( $Y_2 - Y_1$ ).

By loading the walker in lateral direction, it is observed that the wheel motors begin to slip for  $F_y > 80$  N. Therefore,  $F_{ymax} = 80$  N.

Additionally, the maximum damping range is limited by the width of the walker. The average separation between a person's feet is approximately 30 cm. Thus, if the walker needs to provide support when the patient is in mid-swing (worst case), there is a maximum of 20 cm clearance between the walker and the person's other foot (figure 7.3). A safe estimate for  $Y_2 - Y_1$  is used as .15 m.

Therefore,

$$K > \frac{F_{ymax}}{|Y_2 - Y_1|} \approx 530N/m \quad (7.9)$$

Upon trials, comfortable values for  $|Y_1|$  and  $b$  were found to be .05 cm and 900 Ns/m respectively.

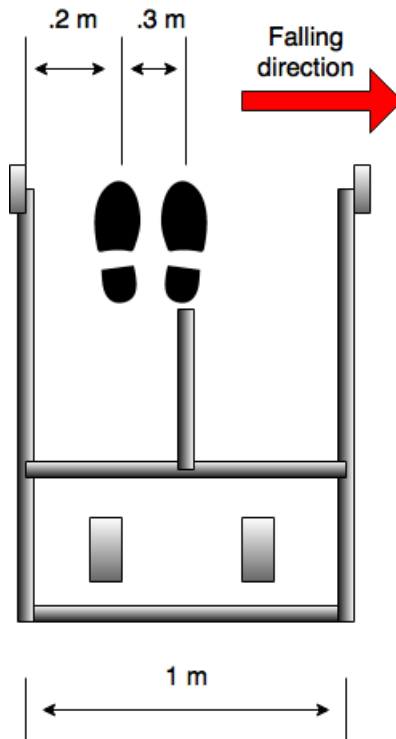


FIGURE 7.3: Patient falling towards right.

### 7.3 Comments on Safety Zone

The implementation of force-tunnel based on safety zone criteria shows the feasibility of the force-tunnel. However, this criteria imposes some restrictions walker's mobility as it is very difficult to move sideways using this approach. Additionally, it limits the radius of curvature when it is required to take a turn. These problems limits the applicability of force-tunnel for overground robotic walkers. In the next section, force-tunnel method is made more feasible by improving the stability criterion and a new 'Stable Gait Criterion' (SGC) is proposed which removes the current limitations of the force-tunnel.

## 7.4 Stable Gait criterion

A reliable fall detection mechanism is characterized with high sensitivity and specificity i.e. it should have large true positives and few false positives. In this work, a ‘Stable Gait Criterion’ is proposed which exploits the key features of the human gait to efficiently identify the instances of gait imbalance in real-time.

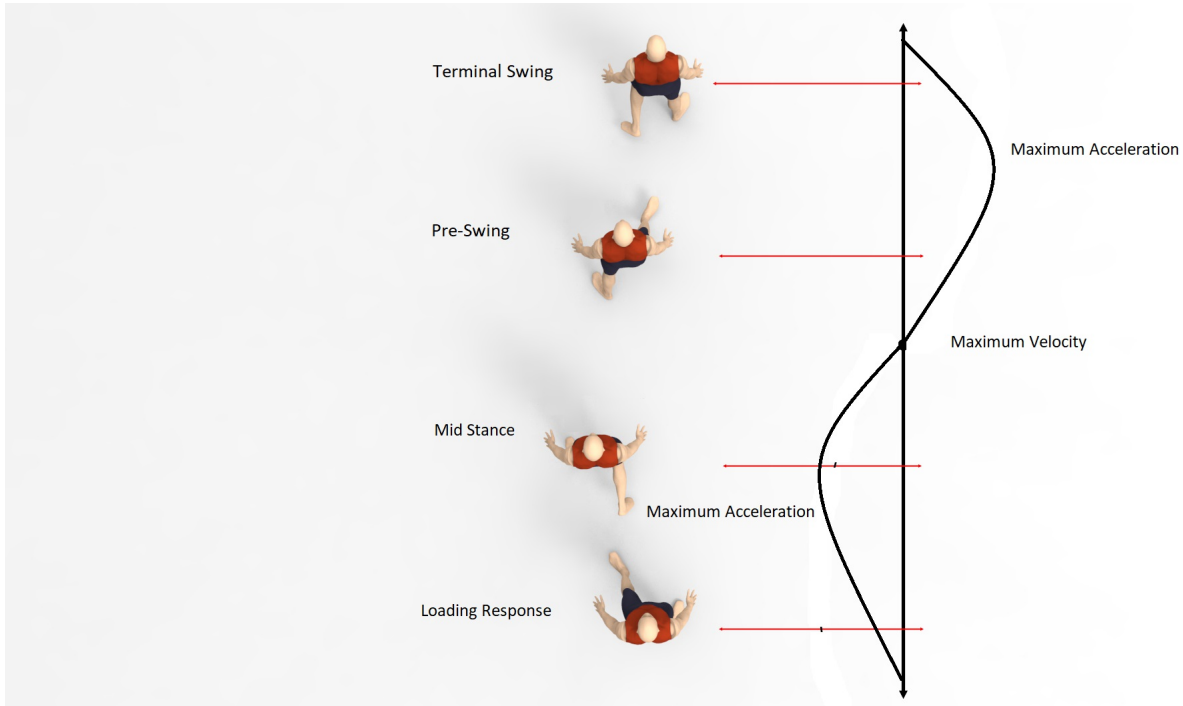


FIGURE 7.4: Lateral trajectory of torso while walking

Figure 7.4 shows the path curve of the center of gravity in the frontal plane during various gait phases. Due to alternating stance and swing phases, the center of gravity(COG) performs periodic motion in the lateral direction [23][5][21]. Figure 7.5 shows the lateral motion of COG of an actual subject while walking forwards in a straight line. The points A and B indicate the interval of a gait cycle in both figures 7.4 and 7.5.

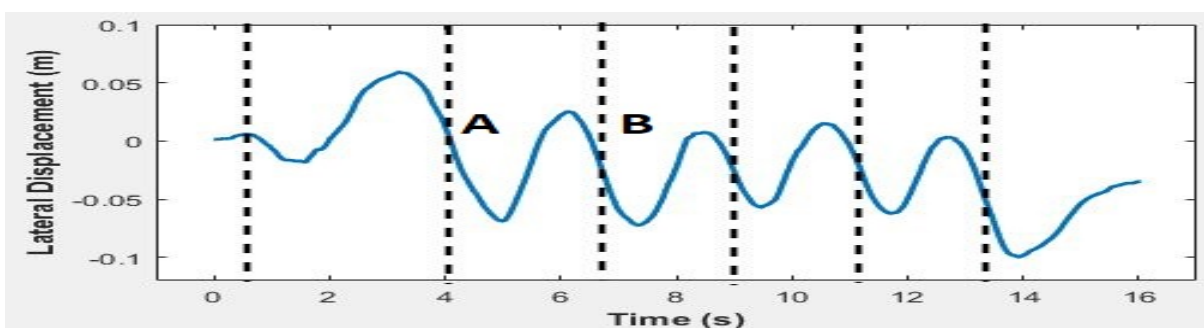


FIGURE 7.5: COG lateral trajectory of a subject.

In this work, the unique nature of the centre of gravity's trajectory in lateral direction is modelled using a function  $f(t)$  which has the following properties.

- $f(t)$  is continuously periodic function
- $f(t)$  has exactly one local maxima and minima in an interval.

Clearly our model of COG's trajectory is more generalized than the traditional sinusoidal models present in the literature. Several studies on the bio-mechanics of fall of stroke patients indicate that the smooth periodic motion of COG is violated at the instance of a fall. Therefore, a criterion can be developed to detect a fall by observing the perturbations in the usual COG trajectory. In this work, we used the model  $f(t)$  of gait trajectory to develop the SGC criterion to detect the fall instance. The following lemma proves the existence of a function  $g(t)$  which is used as the definition of SGC.

**Lemma 7.1.** *Let  $f : \mathbb{R} \rightarrow \mathbb{R}$  be a continuously periodic function with period  $T$ . If  $f(t)$  has exactly one local maxima and minima in  $[t, t + T]$ , then  $\exists g : \mathbb{R} \rightarrow \mathbb{R}$  such that*

$$g(t) = (f(t) - f(t_m)) \frac{d^2 f(t)}{dt^2} \leq 0 \quad \forall t \text{ where,}$$

$$t_m = \begin{cases} \max_t(\frac{df(t)}{dt}), & t \in [\min_t(f(t)), \max_t(f(t))] \\ \min_t(\frac{df(t)}{dt}), & t \in [\max_t(f(t)), \min_t(f(t))] \end{cases}$$

Proof: Let  $t_{min}, t_{max} \in [t, t + T]$  be the respective time instants of local minima and maxima of  $f(t)$ . Without loss of generality, we can assume  $t_{min} \leq t_{max}$ . Therefore, by definition

$$\left. \frac{d^2 f(t)}{dt^2} \right|_{t=t_{min}} \geq 0 \quad (7.10)$$

$$\left. \frac{d^2 f(t)}{dt^2} \right|_{t=t_{max}} \leq 0 \quad (7.11)$$

Then, by continuous value theorem,  $\exists t_m \in [t_{min}, t_{max}]$  such that

$$\left. \frac{d^2 f(t)}{dt^2} \right|_{t=t_m} = 0 \quad (7.12)$$

Since  $f(t)$  attains exactly one maxima and minima in  $[t, t + T]$

$$\frac{d^2 f(t)}{dt^2} \geq 0, \quad t_{min} \leq t \leq t_m \quad (7.13)$$

$$\frac{d^2 f(t)}{dt^2} \leq 0 , \quad t_m \leq t \leq t_{max} \quad (7.14)$$

Additionally, for  $t_{min} \leq t \leq t_{max}$ ,  $f(t)$  is monotonically increasing.

$$\implies f(t_{min}) \leq f(t_m) \leq f(t_{max}) \quad (7.15)$$

Thus, from (4), (5) and (6) we get

$$g(t) = (f(t) - f(t_m)) \frac{d^2 f(t)}{dt^2} \leq 0 , \quad t_{min} \leq t \leq t_{max} \quad (7.16)$$

Now consider the interval  $[t_m, t_m + T]$ . We have,

$$\frac{d^2 f(t)}{dt^2} \Big|_{t=t_{min}+T} \geq 0 \quad (7.17)$$

Therefore, by continuous value theorem  $\exists t_{m'} \in [t_m, t_m + T]$  such that

$$\frac{d^2 f(t)}{dt^2} \Big|_{t=t_{m'}} = 0 \quad (7.18)$$

Since  $f(t)$  attains exactly one maxima and minima in  $[t_m, t_m + T]$

$$\frac{d^2 f(t)}{dt^2} \leq 0 , \quad t_{max} \leq t \leq t_{m'} \quad (7.19)$$

$$\frac{d^2 f(t)}{dt^2} \geq 0 , \quad t_{m'} \leq t \leq t_{min} + T \quad (7.20)$$

Since,  $f(t)$  is monotonically decreasing in  $[t_{max}, t_{min} + T]$

$$\implies f(t_{max}) \geq f(t_{m'}) \geq f(t_{min} + T) \quad (7.21)$$

Thus, from (10),(11) and (12) we get,

$$g(t) = (f(t) - f(t_{m'})) \frac{d^2 f(t)}{dt^2} \leq 0 , \quad t_{max} \leq t \leq t_{min} + T \quad (7.22)$$

Hence we prove the Lemma. The Lemma 2.1 provides a criteria to check the instantaneous gait stability. The condition  $g(t) \leq 0$  is always satisfied while walking normally. In other words,  $g(t) \leq 0$  symbolizes a ‘stable gait’. The instant when  $g(t) > 0$  it is assumed that the stability of the gait is lost and safety control needs to be enabled. Since, it is difficult to arrive at an estimate of  $t_m$ . The symmetric nature of human gait is used to arrive at a good heuristic to estimate  $f(t_m)$ . In this work an ‘Exponential Moving Average (EMA)’ is used as the heuristic

for estimation of  $f(t_m)$  over the entire duration of rehabilitation therapy.

We thus, arrive at the working definition of ‘Stable Gait Criterion’ :

$$g(t) = (f(t) - \hat{f}) \frac{d^2 f(t)}{dt^2} \leq \delta \quad (7.23)$$

Where  $f(t)$  is the lateral displacement of torso,  $\hat{f}$  is the EMA of  $f(t)$  and  $\delta > 0$  is used to accommodate some noise. In this work an EMA with time constant equal to step time is used and  $\delta = .01 m^2/s^2$ . Note that the value of  $\hat{f}$  is updated only when  $g(t) \leq \delta$ .

The efficacy of SGC was tested by performing fall detection on a total of five subjects. Figure 7.6 shows the lateral displacement of five patients along with value of SGC flag over throughout their forward motion. The SGC flag is set to one at the instance SGC criterion is violated i.e.  $g(t) > \delta$ . The abrupt lateral displacement around  $x = 3.3m$  represents the falling instance. Clearly, the SGC detects the fall with very less latency in all five test cases. Additionally, there are no false positives by SGC while walking normally. Thus figure 7.6 demonstrates that SGC can be used as an effective trigger for safety control.

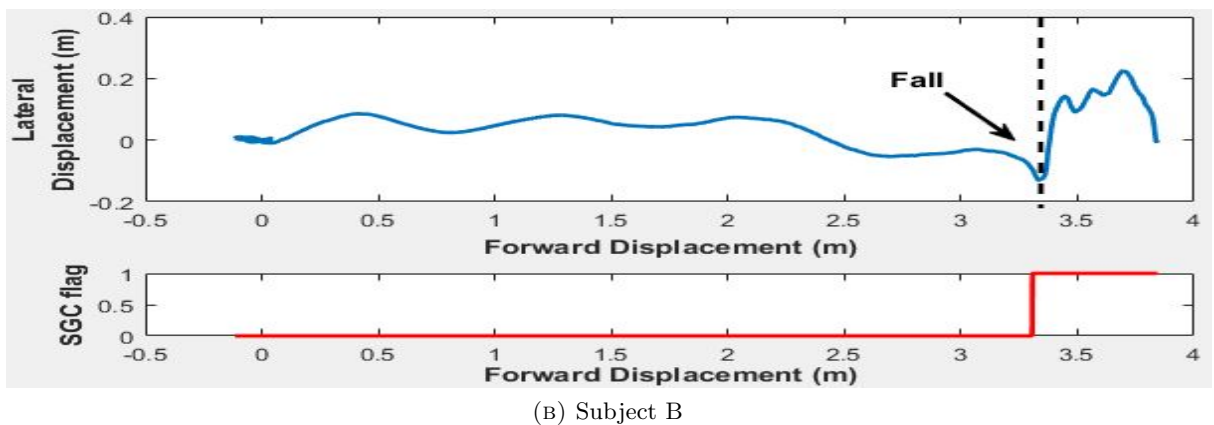
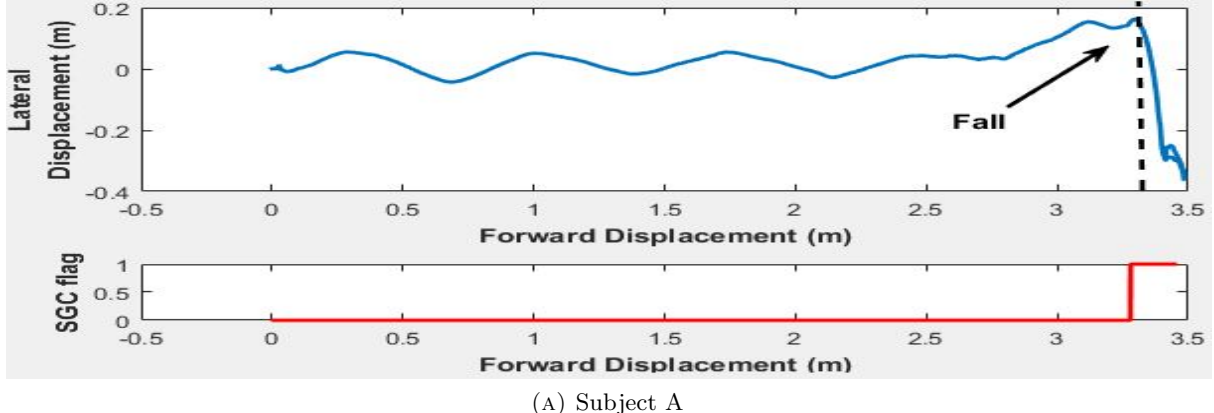


FIGURE 7.6: Transverse trajectory and SGC flag for detecting fall instance

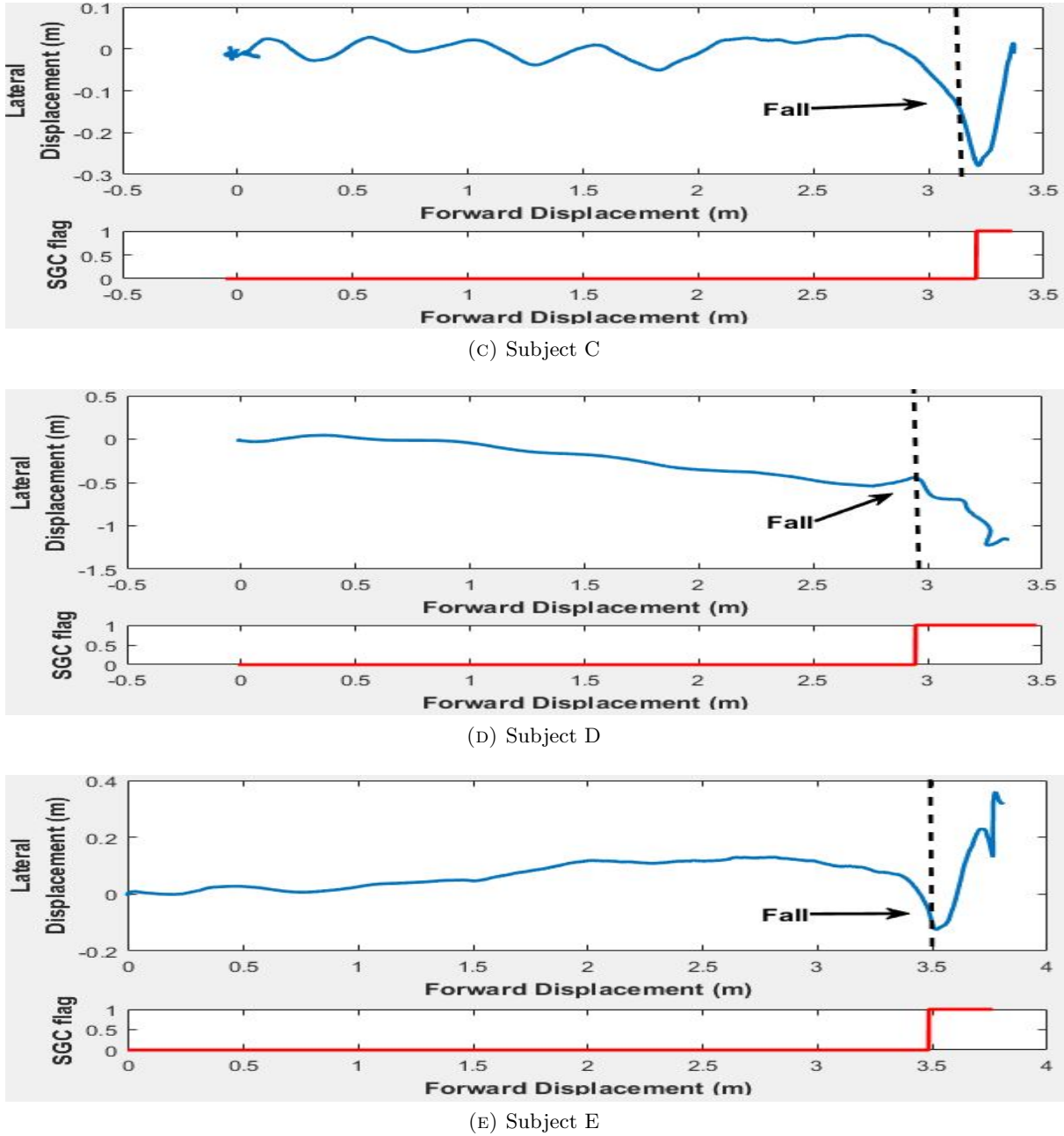


FIGURE 7.6: Transverse trajectory and SGC flag for detecting fall instance

The force-tunnel is implemented using a spring-damper system in forward and lateral directions as shown in figure 7.7. The spring-damper system is enabled the moment gait instability is detected. Under normal operation these dampers remain disabled and only regular admittance control of walker is executed. Here,  $F_{x\text{support}}$  and  $F_{y\text{support}}$  are the supporting force of dampers in forward and lateral directions respectively. The spring and damping coefficients are denoted by  $K$  and  $b$  respectively.

The dynamic equations to followed by the walker are piece-wise defined for the cases  $g \leq \delta$  and  $g > \delta$ .

For  $g(t) \leq \delta$ :

$$M_0\ddot{x} + b_0\dot{x} = F_x \quad (7.24)$$

$$M_0\ddot{y} + b_0\dot{y} = F_y \quad (7.25)$$

For  $g(t) > \delta$ :

$$M_0\ddot{x} + b_0\dot{x} = F_x - F_{x_{support}}(x) \quad (7.26)$$

$$M_0\ddot{y} + b_0\dot{y} = F_y - F_{y_{support}}(y) \quad (7.27)$$

Where,

$$F_{x_{support}}(x) = b\dot{x} + K(x - x^*) \quad (7.28)$$

$$F_{y_{support}}(y) = b\dot{y} + K(y - y^*) \quad (7.29)$$

The quantities  $x^*$ ,  $y^*$  are respective values of  $x$  and  $y$  at the instance safety control is triggered. Here  $M_0$  and  $b_0$  represent admittance parameters in the absence of safety control.

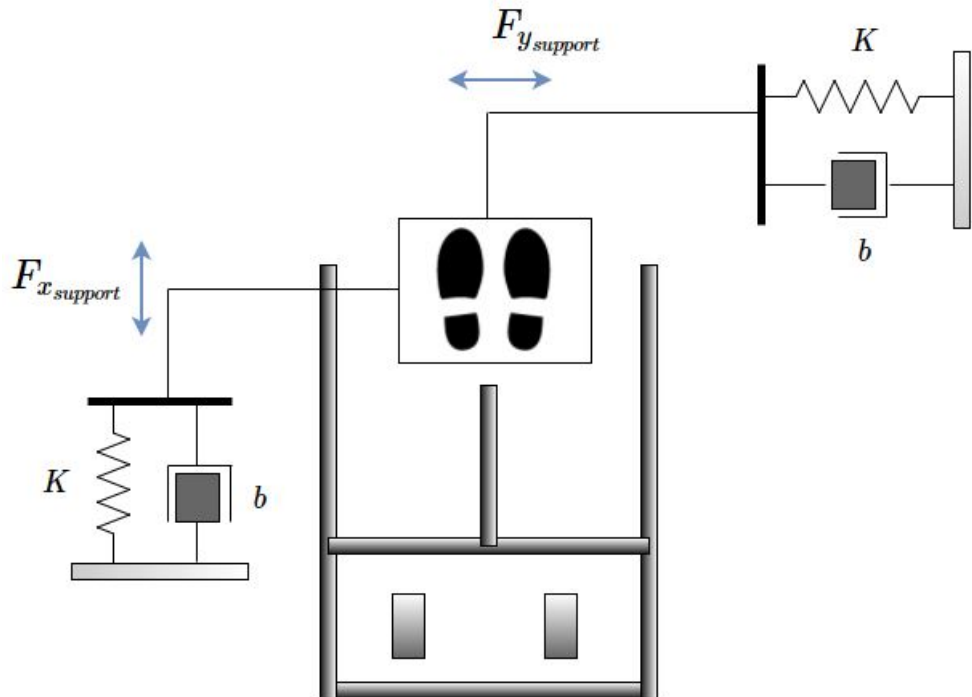


FIGURE 7.7: Spring-Damper system for Force-Tunnel

# **Chapter 8**

## **Results**

The effectiveness of SGC criterion have already been discussed in Chapter 7. The performance of the proposed support scheme by the means of force-tunnel is determined in terms of the following parameters:

- Response time.
- Critical distance.

The performance of safety control subject to these parameters is discussed in the following subsections.

## 8.1 Response time.

Response time of the supporting action is defined as the time taken by the force tunnel to bring the subject to rest after the gait instability is detected. In figure 8.2 the velocity (blue) damping by the force tunnel is shown for five subjects. The zero velocity level is shown in red. The vertical dash line (black) marks the time at which gait instability is detected.

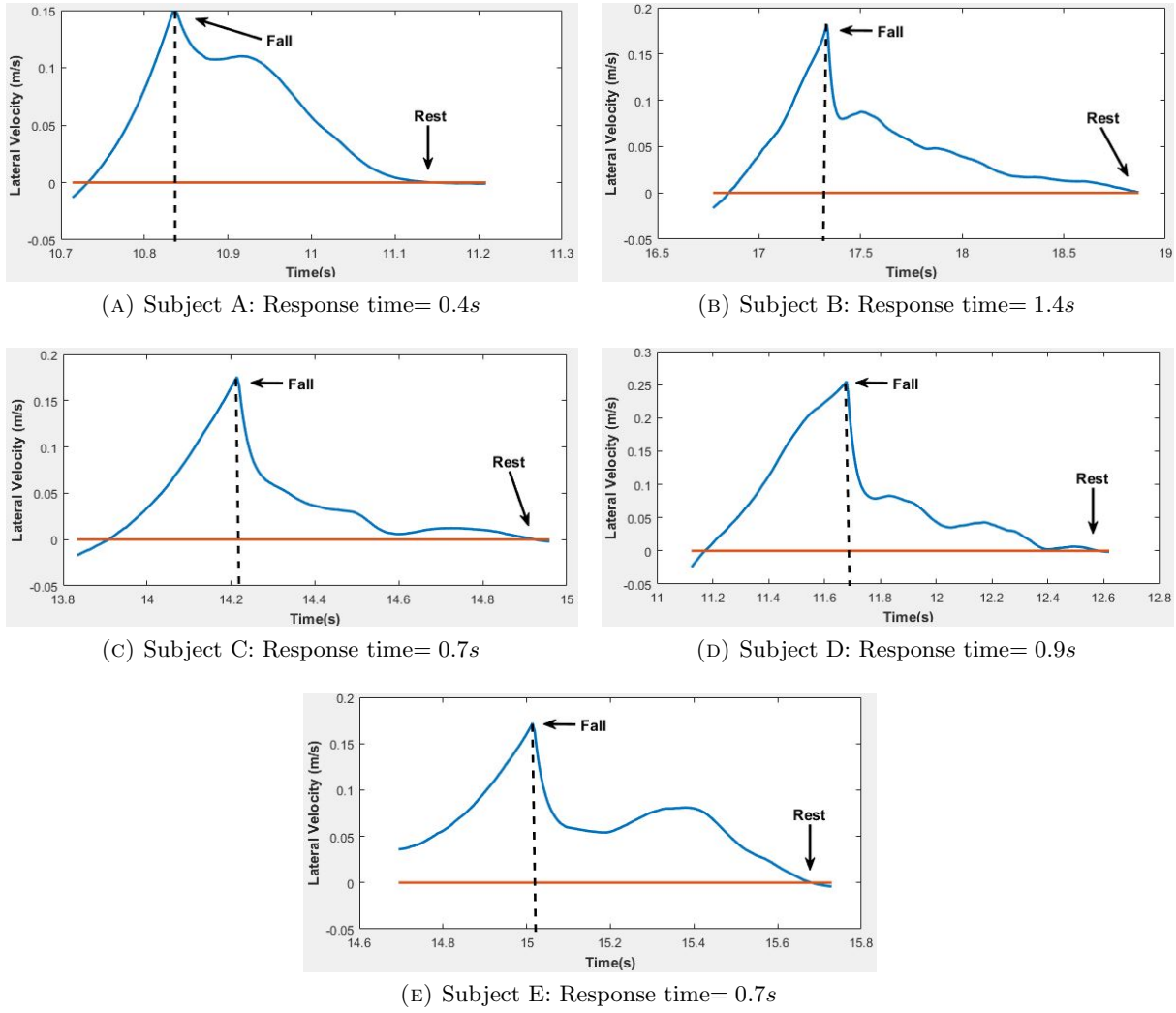


FIGURE 8.1: Response time of supporting action.

The average response time of force-tunnel is found to be around 0.8s which is very low. This implies that the force-tunnel can quickly bring the falling patient to rest thereby preventing any injuries.

## 8.2 Critical distance.

Once gait instability is detected, it is important to bring the subject to rest without falling over a large distance. ‘Critical distance’ is defined as the maximum distance over which the subject falls during supporting action before coming to rest. The figure 8.2 (a)-(e) contrasts the lateral displacements of five subjects while force-tunnel is on (blue) and off (red). Zero displacement level is shown in black.

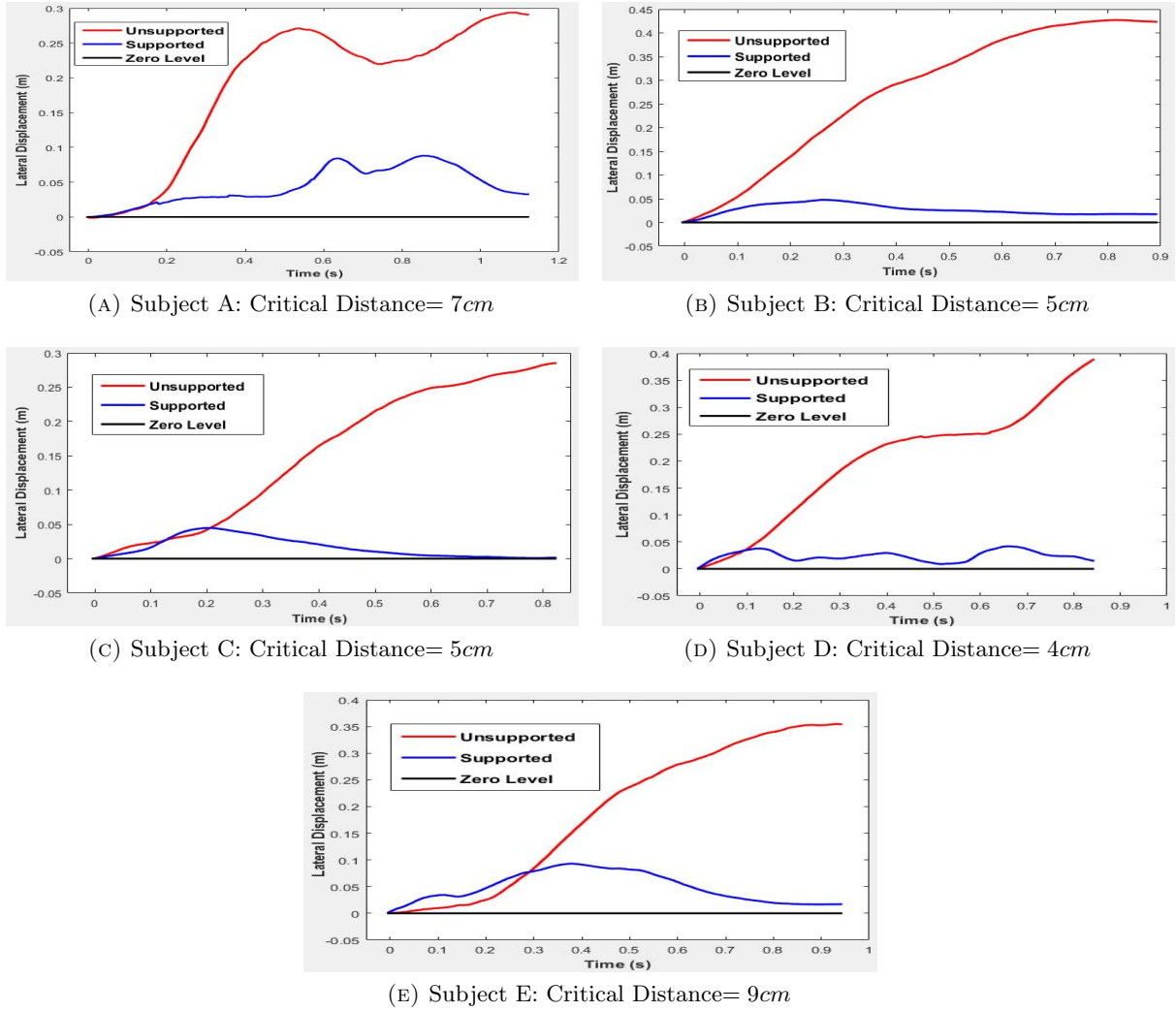


FIGURE 8.2: Response time of supporting action.

The average critical distance of force-tunnel is found to be around 6cm which is very little. This implies that the force-tunnel can provide the adequate supporting force without deviating a lot from the original path.

# Chapter 9

## Conclusions

There are several key points to note about the proposed safety control based on SGC and force-tunnel especially when compared to previously reported methods based on the concept of ‘Safety-Zone’.

- Firstly, using Kalman filter has enhanced state estimation of walker. This has lead to an improvement in the detection of gait instability.
- The proposed ‘Stable Gait Criterion’ (SGC) has been shown to be a reliable mechanism to detect gait instability. It is sensitive even towards very low perturbations in user’s gait. It also has a high specificity wherein instances of false positives are very rare.
- In contrast to the previously reported ‘safety zone’ (which utilized lateral displacement for triggering), SGC does not restrict the regular functioning of the walker. With SGC, the walker is able to span the entire transverse plane and also take sharp turns without having false positives about gait instability. Thus the proposed safety control acts independently of the regular walker control and can in-fact be implemented as a separate real-time thread.
- In the proposed force-tunnel, support to the user is provided in both forward and lateral directions which has greatly increased the net-supporting force. With this enhanced supporting force it is now possible to fully prevent fall of the user which was not possible before.
- The five subjects who were involved in this study showed confidence about the walker’s ability to provide them adequate support when required and reported that it did not interfere with their regular use of the walker.

Based on the above discussion we can conclude that the proposed safety control is a useful addition to the current walker control.

## 9.1 Future Work

In future several different methods of detecting gait instability. Use of IMU system can be investigated. Non-invasive EMG signals can also be used for detecting patterns of gait instability in the user.

# Bibliography

- [1] Yves Allemand et al. “Design of a new lower extremity orthosis for overground gait training with the WalkTrainer”. In: *Rehabilitation Robotics, 2009. ICORR 2009. IEEE International Conference on*. IEEE. 2009, pp. 550–555.
- [2] Mohamed RS Amar. “Estimation of mechanical properties of soft tissue subjected to dynamic impact”. In: (2010).
- [3] Sai K Banala et al. “Robot assisted gait training with active leg exoskeleton (ALEX)”. In: *IEEE Transactions on Neural Systems and Rehabilitation Engineering* 17.1 (2009), pp. 2–8.
- [4] Sai K Banala et al. “Robot assisted gait training with active leg exoskeleton (ALEX)”. In: *IEEE Transactions on Neural Systems and Rehabilitation Engineering* 17.1 (2009), pp. 2–8.
- [5] Aline Araujo do Carmo, Ana Francisca Rozin Kleiner, and Ricardo ML Barros. “Alteration in the center of mass trajectory of patients after stroke”. In: *Topics in stroke rehabilitation* 22.5 (2015), pp. 349–356.
- [6] Pei-Hao Chen et al. “Gait disorders in Parkinson’s disease: assessment and management”. In: *International Journal of Gerontology* 7.4 (2013), pp. 189–193.
- [7] Gery Colombo et al. “Treadmill training of paraplegic patients using a robotic orthosis”. In: *Journal of rehabilitation research and development* 37.6 (2000), p. 693.
- [8] Iñaki Díaz, Jorge Juan Gil, and Emilio Sánchez. “Lower-limb robotic rehabilitation: literature review and challenges”. In: *Journal of Robotics* 2011 (2011).
- [9] E Dietrichs. “Brain plasticity after stroke—implications for post-stroke rehabilitation”. In: *Tidsskrift for den Norske laegeforening: tidsskrift for praktisk medicin, ny raekke* 127.9 (2007), pp. 1228–1231.
- [10] Bruce H Dobkin. “An overview of treadmill locomotor training with partial body weight support: a neurophysiologically sound approach whose time has come for randomized clinical trials”. In: *Neurorehabilitation and neural repair* 13.3 (1999), pp. 157–165.

- [11] Vincent Duchaine and Clément Gosselin. “Safe, stable and intuitive control for physical human-robot interaction”. In: *Robotics and Automation, 2009. ICRA '09. IEEE International Conference on*. IEEE. 2009, pp. 3383–3388.
- [12] Susanna Freivogel et al. “Gait training with the newly developed ‘LokoHelp’-system is feasible for non-ambulatory patients after stroke, spinal cord and brain injury. A feasibility study”. In: *Brain Injury* 22.7-8 (2008), pp. 625–632.
- [13] Alan S Go et al. “Heart disease and stroke statistics—2014 update: a report from the American Heart Association”. In: *Circulation* 129.3 (2014), e28.
- [14] Saryn R Goldberg and Steven J Stanhope. “Sensitivity of joint moments to changes in walking speed and body-weight-support are interdependent and vary across joints”. In: *Journal of biomechanics* 46.6 (2013), pp. 1176–1183.
- [15] Patricia A Goldie, Thomas A Matyas, and Owen M Evans. “Deficit and change in gait velocity during rehabilitation after stroke”. In: *Archives of physical medicine and rehabilitation* 77.10 (1996), pp. 1074–1082.
- [16] Zhao Guo, Haoyong Yu, and Yue H Yin. “Developing a mobile lower limb robotic exoskeleton for gait rehabilitation”. In: *Journal of Medical Devices* 8.4 (2014), p. 044503.
- [17] S Hesse et al. “Treadmill training with partial body weight support compared with physiotherapy in nonambulatory hemiparetic patients”. In: *Stroke* 26.6 (1995), pp. 976–981.
- [18] Stefan Hesse, Dietmar Uhlenbrock, et al. “A mechanized gait trainer for restoration of gait”. In: *Journal of rehabilitation research and development* 37.6 (2000), pp. 701–708.
- [19] Stefan Hesse et al. “Restoration of gait in nonambulatory hemiparetic patients by treadmill training with partial body-weight support”. In: *Archives of physical medicine and rehabilitation* 75.10 (1994), pp. 1087–1093.
- [20] Barbro B Johansson. “Brain plasticity and stroke rehabilitation”. In: *Stroke* 31.1 (2000), pp. 223–230.
- [21] T Jurcevic Lulic and O Muftic. “Trajectory of the human body mass centre during walking at different speed”. In: *DS 30: Proceedings of DESIGN 2002, the 7th International Design Conference, Dubrovnik*. 2002.
- [22] Bilal Komati et al. “Explicit force control vs impedance control for micromanipulation”. In: *ASME 2013 International Design Engineering Technical Conferences and Computers and Information in Engineering Conference*. American Society of Mechanical Engineers. 2013, V001T09A018–V001T09A018.
- [23] TE Lockhart. “Biomechanics of Human Gait—Slip and Fall Analysis”. In: () .

- [24] Haifa Mehdi and Olfa Boubaker. "Stiffness and impedance control using Lyapunov theory for robot-aided rehabilitation". In: *International Journal of Social Robotics* 4 (2012), pp. 107–119.
- [25] Nirut Naksuk. "The implementation of a natural admittance controller on an industrial robot". MA thesis. Case Western Reserve University, 2001.
- [26] Sandra J Olney and Carol Richards. "Hemiparetic gait following stroke. Part I: Characteristics". In: *Gait & posture* 4.2 (1996), pp. 136–148.
- [27] James Patton et al. "KineAssist: design and development of a robotic overground gait and balance therapy device". In: *Topics in stroke rehabilitation* 15.2 (2008), pp. 131–139.
- [28] Keir G Pearson. "Generating the walking gait: role of sensory feedback". In: *Progress in brain research* 143 (2004), pp. 123–129.
- [29] Ian H Robertson and Jaap MJ Murre. "Rehabilitation of brain damage: brain plasticity and principles of guided recovery." In: *Psychological bulletin* 125.5 (1999), p. 544.
- [30] Jaydeep Roy and Louis L Whitcomb. "Adaptive force control of position/velocity controlled robots: Theory and experiment". In: *IEEE Transactions on Robotics and Automation* 18.2 (2002), pp. 121–137.
- [31] Mark W Spong, Seth Hutchinson, and Mathukumalli Vidyasagar. *Robot modeling and control*. Vol. 3. Wiley New York, 2006.
- [32] Jan F Veneman et al. "Design and evaluation of the LOPES exoskeleton robot for interactive gait rehabilitation". In: *IEEE Transactions on Neural Systems and Rehabilitation Engineering* 15.3 (2007), pp. 379–386.
- [33] Luigi Villani and Joris De Schutter. "Force control". In: *Springer handbook of robotics*. Springer, 2016, pp. 195–220.
- [34] PT Vivian Weerdesteyn PhD et al. "Falls in individuals with stroke". In: *Journal of rehabilitation research and development* 45.8 (2008), p. 1195.
- [35] Ping Wang, KH Low, and AH McGregor. "A subject-based motion generation model with adjustable walking pattern for a gait robotic trainer: NaTure-gaits". In: *Intelligent Robots and Systems (IROS), 2011 IEEE/RSJ International Conference on*. IEEE. 2011, pp. 1743–1748.
- [36] Kelly P Westlake and Carolynn Patten. "Pilot study of Lokomat versus manual-assisted treadmill training for locomotor recovery post-stroke". In: *Journal of neuroengineering and rehabilitation* 6.1 (2009), p. 18.
- [37] David A Winter. *Biomechanics and motor control of human gait: normal, elderly and pathological*. 1991.
- [38] Shelten G Yuen et al. "Force tracking with feed-forward motion estimation for beating heart surgery". In: *IEEE Transactions on Robotics* 26.5 (2010), pp. 888–896.